Reviewed Preprint
v1 • July 14, 2025
Not revised

Reviewed Preprint
v2 • May 1, 2026
Revised by authors

Hippocampal single-cell RNA Atlas of chronic methamphetamine abuse-induced cognitive decline in mice

Hai Qiu[1], Xia Yue[1], Yuebing Huang[1], Ziling Meng[1], Jiahong Wang[2] ✉, Dongfang Qiao[3] ✉

[1]School of Forensic Medicine, Southern Medical University., Guangzhou, China • [2]Cancer Research Institute, School of Basic Medical Sciences, Southern Medical University, Guangzhou, China • [3]School of Forensic Medicine, Southern Medical University, Guangzhou Key Laboratory of Forensic Multi-Omics for Precision Identification, Guangzhou, China

For correspondence:
wjh1987@smu.edu.cn
qiaodf@smu.edu.cn

Competing interests: No competing interests declared

Funding: See page 26

Reviewing editor: Jihwan Park, Gwangju Institute of Science and Technology, Republic of Korea

eLife Assessment

The authors proposed two hypotheses: first, that methamphetamine induces neuroinflammation, and second, that it alters neuronal stem cell differentiation. These are **valuable** hypotheses, and the authors provided in vivo observations of the methamphetamine response in mice. However, concerns about data interpretation, and the current evidence is **incomplete**, requiring further experimental validation.

https://doi.org/10.7554/eLife.106940.2.sa2

Abstract

Background Chronic methamphetamine abuse leads to cognitive decline, posing a significant threat to human health and contributing to loss of productivity. However, the intricate and multifaceted mechanisms underlying methamphetamine-induced neurotoxicity have impeded the development of effective therapeutic interventions.

Methods To establish a mouse model of cognitive decline induced by chronic methamphetamine exposure, we employed a large sample size and conducted two behavioral tests (Y-maze and novel object recognition test) at 2 and 4 weeks post-exposure. Subsequently, single-cell RNA sequencing was utilized to delineate the mRNA expression profiles of individual cells within the hippocampus.

Comprehensive bioinformatics analyses, including cell clustering and identification, differential gene expression analysis, cellular communication analysis, pseudotemporal trajectory analysis, and transcription factor regulation analysis, were performed to elucidate the cellular-level changes in mRNA profiles caused by chronic methamphetamine exposure.

Results Our findings demonstrated impairments in working memory, spatial cognition, learning, and cognitive memory. After 4 weeks of behavioral testing, we identified diverse cell types in the hippocampi of METH- and saline-treated mice through scRNA-seq, including glial cells, stromal cells, vascular cells, and immune cells. We observed that methamphetamine exerts cell-specific effects on gene expression changes associated with neuroinflammation, blood-brain barrier disruption, neuronal support dysfunction, and immune dysregulation. Furthermore, cross-talk analysis revealed extensive alterations in cellular communication patterns and signal changes within the hippocampal microenvironment induced by methamphetamine exposure. Pseudotime analysis predicted hippocampal neurogenesis disorders and identified key regulatory genes implicated in chronic methamphetamine abuse.

Transcription factor analysis uncovered regulators and pathways linked to astrocyte-mediated neuroinflammation, endothelial junction integrity, microglial synaptic remodeling, and

oligodendrocyte-supported neuronal cell bodies and axons. Additionally, it highlighted the role of neural precursor cells in various forms of neurodegeneration.

Conclusions This study establishes a robust mouse model of cognitive impairment induced by chronic methamphetamine exposure. It provides valuable biological insights, characterizes the single-cell atlas of the hippocampus, and offers novel directions for investigating neurological damage associated with chronic methamphetamine-induced cognitive decline.

Introduction

Methamphetamine (METH), a widely abused psychostimulant globally, particularly in southeast and east Asia, currently holds the position of being the world's foremost illicitly manufactured synthetic drug. Its detrimental impact on human health, social stability, and economic development is immense(1). METH induces intense euphoria and addiction, while causing significant harm to various tissues and organs, especially the central nervous system. With advancements in productivity and medical standards, research focusing on neuropsychiatric issues associated with chronic METH abuse has become a prominent topic concerning drug users' treatment, recovery, and quality of life. Chronic and regular usage of METH has been proven to result in an array of brain structural abnormalities such as cortical and hippocampal atrophy, nucleus accumbens hypertrophy, as well as decreased gray matter(2–4), leading to neuropsychiatric disorders including neurodegeneration, cognitive deficits, agitation, paranoia, depression, delusions, and schizophrenia. However, due to the wide range of affected targets and complex mechanisms underlying METH's effects, the evolution and interplay of these effects during chronic processes make it challenging to analyze the etiology of these neuropsychiatric diseases.

Extensive clinical and experimental evidences suggest that chronic METH abuse leads to cognitive deficits(5–7), which share similarities with neurodegenerative disorders such as impaired inhibitory control, learning and memory decline, attention decrease, increased pathological protein levels, neurotoxicity, neuroinflammation, and blood-brain barrier (BBB) injury. The hippocampus plays a crucial role in regulating cognitive function as part of the limbic system. Previous studies have demonstrated that METH exerts complex negative effects on the hippocampus beyond its direct impact on dopaminergic and glutamatergic systems(8). It also indirectly affects various cell types within the hippocampus and alters the microenvironment. However, due to the intricate composition of the hippocampus and diverse mechanisms underlying METH's effects, certain impacts on vulnerable cell types and critical signaling pathways may be concealed during chronic exposure, making it challenging to unravel these mechanisms. Currently, there is limited understanding of the specific mechanisms responsible for chronic METH-induced neurotoxicity in the hippocampus leading to cognitive deficits; furthermore, theories explaining this wide range of effects are scarce.

In this study, we employed single-cell RNA sequencing (scRNA-seq) to construct a comprehensive hippocampal atlas of chronic METH abuse-induced cognitive decline in mice. To elucidate the underlying mechanisms by which chronic METH abuse affects the hippocampus and leads to cognitive deficits, we conducted animal behavior tests, performed scRNA-seq analysis with clustering and differential gene expression analyses, investigated cellular cross-talk, examined single-cell trajectories, and analyzed transcription factors. This study provides in vivo evidence of heterogeneous changes in hippocampal cells under chronic METH abuse and contributes to a more robust understanding of the mechanistic basis for cognitive deficits while also bridging previous theories on METH neurotoxicity.

Materials and methods

Animal and Treatments

All mice used were male and on C57BL/6 background. Healthy 7-week-old mice were purchased from the Laboratory Animal Center of Southern Medical University (Guangzhou, China). Mice were quarantined for 2 weeks and then housed in the Central Exhaust Ventilation Cage System (Houhuang experimental equipment technology, Suzhou, China) with 12 hours (h) light/12 h dark cycle in a temperature-(20–22 ℃) and humidity- (45–55%) controlled vivarium and had ad libitum access to water and food. All protocols approved by the Institutional Animal Care and Use Committee in Southern Medical University (Ethical number: L2022125), and consistent with NIH Guidelines for the Care and Use of Laboratory Animals (8th Edition, U.S. National Research Council, 2011). After 1 week for adapting, mice were 10 weeks of age at the start of the experiment. They were randomly divided into two groups, and then treated by saline or METH (National Institutes for the Control of Pharmaceutical and Biological Products, Beijing, China). Mice of METH group were intraperitoneally administered METH dissolved in saline at a incremental dose from 1 up to 10 mg/kg, and the daily dose was evenly divided into two doses at 12-hour intervals, while those of saline control underwent the same way of injection with saline simultaneously. The treatments lasted for 28 days. However the last administration of 12 h before animal behavior tests or sample-collecting would be skipped. For scRNA-seq, we used 20 mice (10 from saline group, 10 from METH group, and each random 2 mice from same cage were composed of 1 sample).

Behavioral Experiments

Behavioral testing of mice used for scRNA-seq experiments followed an established protocol. To minimize any stimulation, mice would be handled for 5 days to be habituated to environment and tester (30 min to environment, 5 min to tester) before behavioral experiments. Less irritating behavioral experiments were used to evaluate in order to minimize impacts on scRNA-seq.

Y-Maze

Y maze test was used to evaluate spontaneous alternation behavior in mice. The Y-maze was made of three arms set at angles of 120°. Its walls are covered with frosted adhesive paper. Mice were placed in the end of fixed arm of Y-maze, then they were allowed to freely explore whole Y-maze for 8-min session while camera system recorded the behavior of mice. The total number of entries of each arm (recognizing that all four legs of mouse entered the arm as the standard for entries), the number of alternations (an alternation is defined as successive entries into the three arms on overlapping triplet sets.), and the ratio of them were regarded as statistical indicators to assess spatial working memory.

Novel Object Recognition Test

Novel object recognition test (NOR) was applied to assess mice recognition memory. The testing room was lit with four LED lights which provide the light intensity of approximately 20 lx in each test box (50 × 50 × 40 cm). Mice were put into test room to habituate for 24h before beginning of test, and would be given 10 min to explore the object-free box and were then returned to their home cage. In training stage, two objects of same appearance were placed at a symmetrical position in test box where mice would explore freely for 10min to be fully acquainted with objects. After training, mice were sent back to their home cage to rest for 30 min. Then in testing stage, they were placed back into original test box with a familiar old object and a novel one at the same place and also allowed to explore freely for 10 min. The familiar object and novel object and their placement were counterbalanced within each group. Camera system was placed above the test box and recorded behaviors of mice in test box for statistics.

The following behaviors were scored as exploration: biting, sniffing, licking, touching the object with the nose or with the front legs, or proximity (≤1 cm) between the nose and the object. If the mouse put its hind legs on objects, or stood on top of the object or completely immobile, exploration was not scored. The preference index for the novel object was calculated as (time spent exploring the new object / the total time spent exploring both objects), and the discrimination index was calculated as (time spent exploring the new object − time spent exploring the familiar old object) / (total time spent exploring both objects). Behavior was scored on video by two observers blinded to the mice's treatment.

Brain Samples Collecting

For scRNA-seq, we used hippocampus tissues of 20 mice (10 from saline group, 10 from METH group, and each random 2 mice from same cage were regarded as 1 sample). Hippocampus collecting was carried out under the guidance of JOVE(8).

After the mice were subjected to 3 min of pre-cooling with PBS for cardiovascular perfusion, whole hippocampus was dissected integrally on icein the shortest time (within 5 min) and preserved in tissue preservation solution (SeekGene, China) at 4℃ for following tissue dissociation.

Cell Preparation for Sing Cell RNA Sequencing

After harvested, tissues were washed in ice-cold RPMI1640 and dissociated using Tissue Dissociation Reagent A (Seekone K01301-30, China) from SeekGene as instructions. DNase I (Sigma 9003-98-9, USA) treatment was optional according to the viscosity of the homogenate. Cell count and viability was estimated using fluorescence Cell Analyzer (Countstar® Rigel S2) with AO/PI reagent after removal erythrocytes (Solarbio R1010, China) and then debris and dead cells removal was decided to be performed or not (Miltenyi Biotec 130-109-398/130-090-101, USA). Finally fresh cells were washed twice in the RPMI1640 and then resuspended at 1×10^6 cells/mL in 1×PBS and 0.04% bovine serum albumin.

Single Cell RNA Sequencing Library Construction and Sequencing

Single-cell RNA-Seq libraries were prepared using Chromium Next GEM Single Cell 3′Reagent Kits v3.1 (10x Genomics Catalog No.1000268, USA). Briefly, appropriate number of cells were mixed with reverse transcription reagent and then loaded to the sample well in Chromium Next GEM Chip G. Subsequently Gel Beads and Partitioning Oil were dispensed into corresponding wells separately in chip. After emulsion droplet generation reverse transcription were performed at 53℃for 45 min and inactivated at 85℃ for 5 min. Next, cDNA was purified from broken droplet and amplified in PCR reaction. The amplified cDNA product was then cleaned, fragmented, end repaired, A-tailed and ligated to sequencing adaptor. Finally, the indexed PCR was performed to amplify the DNA representing 3' polyA part of expressing genes which also contained Cell Bar code and Unique Molecular Index. The indexed sequencing libraries were cleanup with SPRI beads, quantified by quantitative PCR (KAPA Biosystems KK4824) and then sequenced on illumina NovaSeq 6000 with PE150 read length.

Processing the Single Cell RNA Sequencing Data and Date Quality Control

The raw sequencing data was processed by Fastp firstly (Chen, Zhou et al. 2018) to trim primer sequence and low quality bases. And then we employed the Cell Ranger software v7.0 (10X Genomics) obtained from *https://www.10xgenomics.com/support/software/cell-ranger/downloads* to precess sequence data and aligned to mouse mm10 genome in order to obtain gene expression matrix. Subsequently, the gene expression matrices of each sample were obtained and further analyzed using Seurat v.4.4.0. Then we determined effective cells using the following criteria: (a) total UMI counts more than 1000 but less than the 97th percentile for each cell; (b) gene numbers between 1000 and 7000; (c) percentage of mitochondrial genes < 10%; and (d) percentage of

hemoglobin genes < 0.1%. Moreover, we excluded genes expressed in fewer than 3 cells, as well as MALAT1, mitochondrial genes, and hemoglobin genes. And the remaining cells and genes were used for subsequent analysis. Quality control charts are included in SI.4.

Data integration, Dimensionality reduction, and Clustering

After performing quality control and filtering, DoubletFinder v2.0.3 was then employed to identify double cells with an expectation value of doublets calculated as an increase of 0.8% for every 1000 additional cells, pN at 0.25, and pK according to function Find.pk. Library-size normalization was conducted for each cell using the NormalizeData function in Seurat v.4.4.0. The 2000 most variable genes were identified using the FindVariableGenes. Subsequently, all libraries were integrated using Harmony (Ilya Korsunsky et al., 2019) to correct batch effects. ScaleData was applied to regress out variability associated with the numbers of UMIs, followed by dimensionality reduction through RunPCA and RunUMAP (dimensions = 1:20). Finally, clustering of cells was performed using the FindClusters function with a resolution of 0.8 based on the 1:24 dimensions.

Celltype Identifcation

FindAllMarkers was used to compare each cluster to all others to identify canonical cell type-specific marker genes. Each retained marker gene was expressed in a minimum of 25% of cells and at a minimum log fold change threshold of 0.25. The clustering differential expressed genes were considered significant if the adjusted P-value was less than 0.05 and the avg_log2FC was ≥ 0.25. And the clusters were annotated using cell type-specific signatures and marker genes from Cellmarker2.0 and PanglaoDB.

Differentially Expressed Genes (DEGs) analysis and Enrichment Analysis

DEG analysis between cell types was performed following the muscat (v.1.16.0, Crowell et al. 2020) R package pipeline, which facilitates multi-sample, multi-condition comparisons of single-cell RNA-seq data. Genes were ranked by absolute log2 fold-change (log2FC), and those with p-values > 0.05 (adjusted for multiple comparisons) and log2FC < 0.25 were removed. Gene Ontology (GO, *https://www.geneontology.org/*) enrichment analysis of DEGs was implemented by the clusterProfiler R package (Yu et al., 2012). GO terms with corrected P value less than 0.05 were considered significantly enriched by DEGs. Kyoto Encyclopedia of Genes and Genomes database (KEGG, *http://www.genome.jp/kegg/*, Kanehisa et al., 2008) is a database resource for understanding high-level functions and utilities of the biological system, such as cell, organism and ecosystem, from molecular-level information, especially large-scale molecular datasets generated by genome sequencing and other high-through put experimental technologies. We used clusterProfiler R package to test the statistical enrichment of DEGs in KEGG pathways.

Cellular Cross-talk Analysis

We utilized the Cellchat (v.1.6.1, Suoqin Jin et al., 2021, *http://www.cellchat.org/*) to analyze the expression abundance of ligand–receptor interactions across hippocampal cell types. The analysis was conducted in accordance with the CellChat user guidelines(9). Cell communication networks were inferred by identifying differentially expressed ligands and receptors between distinct hippocampal cell types. Interaction probabilities at the ligand–receptor level were calculated using the default 'truncatedMean' method, under which the average expression of a signaling gene is set to zero if it is expressed in less than 10% of cells within a given group. The influence of population size was normalized during the calculation of interaction probabilities. Furthermore, L-R interaction probabilities within each signaling pathway were aggregated to compute pathway-level communication probabilities using the function 'computeCommunProbPathway'. Cell–cell communication networks were subsequently summarized by summing the number of interactions or the previously calculated communication probabilities via the function 'aggregateNet'. To compare signaling patterns between METH and Saline groups, we conducted differential expression analysis between METH and Saline samples within each cell type. To ensure

consistency in node size and edge weights across inferred networks from different datasets, we calculated the maximum number of cells per cell group and the maximum interaction counts (or interaction weights) across the two datasets. Differential and conserved networks were identified based on their functional roles, and their divergence indicators were computed accordingly. We also compared outgoing, incoming, and overall signaling patterns between the two datasets and across different cell types. To identify major signaling roles of specific cell types within defined pathways, we visualized the computed centrality scores using heatmaps. Discrepant ligands and receptors were identified if both the log-fold change (logFC) and the percentage of cells expressing the gene in a given cluster exceeded 0.1 in either sender or receiver cells, as determined by the function 'identifyOverExpressedGenes'. Finally, differentially expressed L-R pairs were extracted based on upregulated or downregulated ligands and receptors in METH compared to Saline groups.

Pseudotime analysis

Monocle2(10) (version 2.18.0) was utilized for pseudotime trajectory analysis to elucidate the differentiation trajectory of cell development. The UMI matrix was extracted from the Seurat object and used to create a new object with the 'newCellDataSet' function. For the trajectory analysis, the 2000 most highly variable genes were selected, followed by dimensionality reduction with the DDRTree method and cell ordering with the 'orderCells' function. Genes exhibiting significant changes along the pseudotime trajectory were identified using the 'differentialGeneTest' function. The 'plot_cell_trajectory' function was utilized to visualize the trajectory in a two-dimensional space, effectively presenting the cell differentiation state. The observed branching patterns in the single-cell trajectories reflect distinct biological functions, which were inferred based on gene expression dynamics during development.

SCENIC analysis

SCENIC analysis was utilized to explore key transcription factors (TFs) that regulate inter-cell type differences. The analysis was conducted using pySCENIC with default parameters, following the established protocol(11). Initially, a co-expression network was constructed using GRNBoost2. Subsequently, regulons for each transcription factor were inferred using the RcisTarget motif databases(12) (mm10-refseq-r80-10kb-up-and-down-tss.mc9nr.feather and mm10-refseq-r80-500bp-up-and-100bp-down-tss.mc9nr.feather). Activity scores (AUC values) for each TF regulon in individual cells were calculated using AUCell. Significant TF regulons associated with specific cell types were identified using the 'FindAllMarkers' function in Seurat. The regulatory networks involving transcription factors and their target genes were further visualized and analyzed using Cytoscape (v3.10.1). Additionally, functional enrichment analyses of the target genes were conducted using the clusterProfiler R package, as previously described.

Statistical Analysis

For the experimental data, statistical analyses and graphical visualization were performed using GraphPad Prism software (version 8.0.2, USA). The normality of data distribution was assessed using the Shapiro – Wilk test, although the sample size in each group was close to 30, which is considered relatively large. Results from the Y-maze and NOR tests were presented as mean ± SEM. Between-group differences in the alternation triplet of the Y-maze, as well as the discriminant index, preference index, total exploration time, and frequency of interactions with new and old objects within 10 minutes, were analyzed using the unpaired Student's t-test. A P value < 0.05 was considered statistically significant, and all statistical tests were two-tailed.

For the single-cell RNA sequencing data, statistical analyses and figure generation were conducted using R (v4.3.1). Bioinformatic tools were applied to analyze cellular clustering, differentially expressed genes, functional enrichment, intercellular signaling cross-talk, single-cell trajectory inference, and SCENIC-based regulatory network analysis.

Result

1. Chronic METH exposure led to cognitive decline in adult mice

The construction of the METH chronic exposure mouse model and the arrangement of behavioral experiments are illustrated in Fig.1.A. Adult male mice subjected to chronic METH exposure exhibited significant declines in working memory and spatial cognition, as demonstrated by Y-maze tests conducted at the end of both the second and fourth weeks of administration. In the 2-week test, the mean difference between the METH-treated (n=32) and saline-treated (n=29) groups was -0.1664 (95% CI: -0.2126 to -0.1202, $p < 0.0001$). In the 4-week test, the mean difference was -0.2202 (METH, n=30 vs. Saline, n=29; 95% CI: -0.2728 to -0.1676, $p < 0.0001$) (Fig.1B).

Following chronic METH exposure, NOR tests also revealed impairments in the animals' ability to discriminate novel objects. In the 2-week NOR test, the discrimination index was 0.3119 ± 0.0300 (mean ± SEM) for saline-treated mice (n = 29), compared to 0.1569 ± 0.0462 for METH-treated mice (n = 29). The mean difference in discrimination index between the METH and Saline groups was -0.1550 ± 0.0551 ($p = 0.0068$, 95% CI: -0.2653 to -0.0446) (Fig.1C). The preference index was 0.6559 ± 0.0150 for saline-treated mice and 0.5785 ± 0.0231 for METH-treated mice, resulting in a mean difference of -0.07748 ± 0.0276 ($p = 0.0068$, 95% CI: -0.1327 to -0.0223) (Fig.1C).

The total exploration time for novel objects was 28.36 ± 2.285 seconds in the saline group, compared to 18.38 ± 1.453 seconds in the METH-treated group. The mean difference in total exploration time for novel objects was -9.974 ± 2.708 ($p = 0.0005$). For old objects, the total exploration time was 14.79 ± 1.173 seconds in the saline group and 13.44 ± 1.067 seconds in the METH group, yielding a mean difference of -1.352 ± 1.586 ($p = 0.3976$) (Fig.1D).

Exploration frequency analysis showed that saline-treated mice explored the novel object an average of 25.55 ± 1.565 times, compared to 19.66 ± 1.368 times in the METH group. The mean difference in novel object exploration frequency was -5.897 ± 2.079 ($p = 0.0063$) (Fig.1E). Similarly, the frequency of old object exploration was 19.14 ± 1.359 in the saline group versus 15.41 ± 1.010 in the METH group, with a mean difference of -3.724 ± 1.693 ($p = 0.0320$) (Fig.1E).

Collectively, these findings indicate that following 2 weeks of METH treatment, mice exhibited significant impairments in cognitive and mnemonic functions, as well as reduced exploratory behavior.

In the 4-week NOR test, the discrimination index was 0.3019 ± 0.0389 for the saline group (n = 29), compared to 0.0880 ± 0.0368 for the METH group (n = 29). The mean difference in discrimination index between the METH and saline groups was -0.2139 ± 0.0536 ($p = 0.0002$, 95% CI: -0.3213 to -0.1066) (Fig.1F). The preference index was 0.6510 ± 0.0195 in the saline group and 0.5440 ± 0.0184 in the METH group, resulting in a mean difference of -0.1070 ± 0.0268 ($p = 0.0002$, 95% CI: -0.1606 to -0.0533) (Fig.1F).

The total exploration time for novel objects was 20.04 ± 1.502 seconds in the saline group and 13.05 ± 1.019 seconds in the METH group, yielding a mean difference of -6.996 ± 1.815 ($p = 0.0003$) (Fig.1G). For old objects, the total exploration time was 10.50 ± 0.919 seconds in the saline group and 11.39 ± 1.119 seconds in the METH group, with a mean difference of 0.8922 ± 1.448 ($p = 0.5402$) (Fig.1G).

Exploration frequency for novel objects was 22.10 ± 1.293 in the saline group and 18.52 ± 1.521 in the METH group, resulting in a mean difference of -3.586 ± 1.996 ($p = 0.0778$) (Fig.1H). For old objects, the exploration frequency was 18.10 ± 1.658 in the saline group and 15.03 ± 1.585 in the METH group, with a mean difference of -3.069 ± 2.294 ($p = 0.1864$) (Fig.1H).

These findings indicate that chronic METH exposure leads to a decline in learning and cognitive memory abilities in mice. Although no significant differences in exploration frequency were observed between the METH and saline groups during the 4-week test, the discrimination and preference indexes showed greater statistical significance and further deterioration in the METH group compared to the 2-week test.

These results suggest that prolonged METH exposure may progressively impair cognitive function.

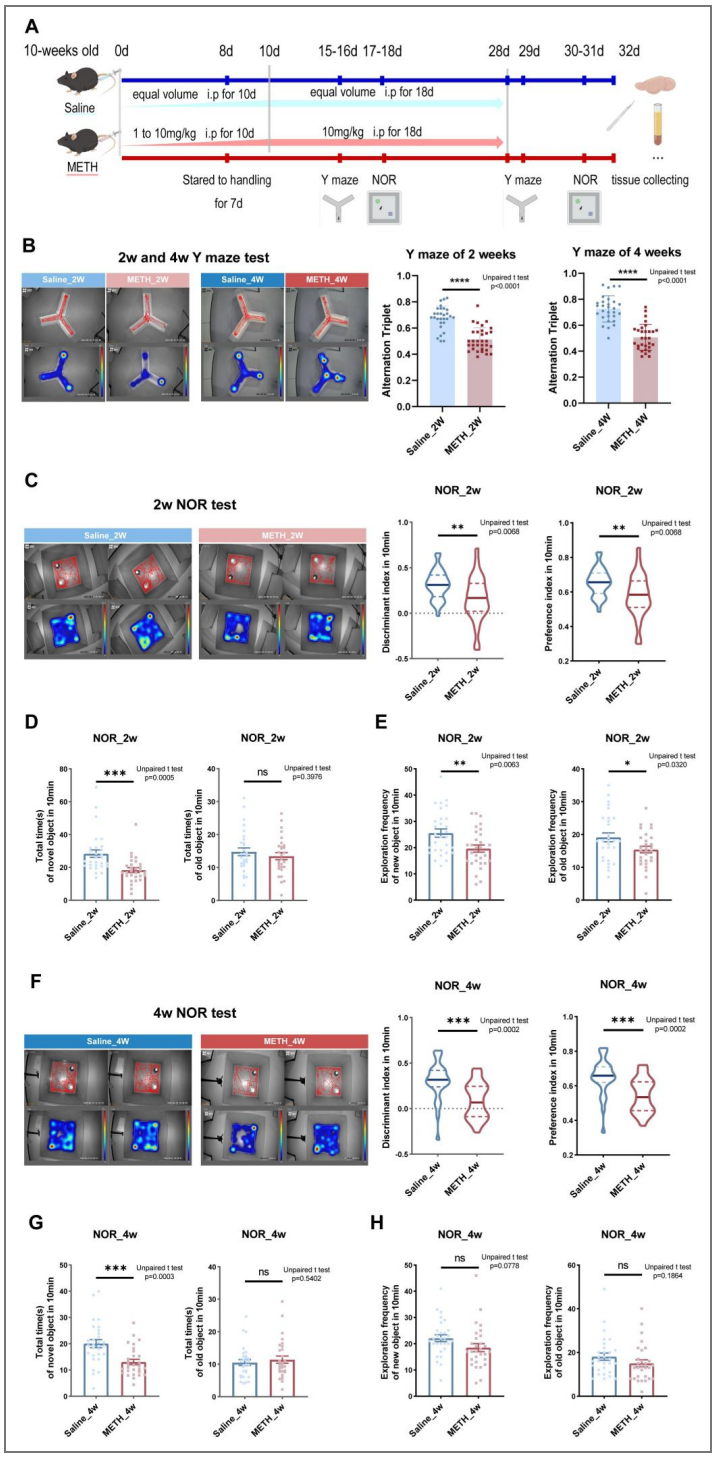

Fig. 1. Mice treatment and result of behaviour tests.

(A) The construction mouse model of chronic METH abuse. (B) The track visualizations and heatmaps of Y maze in 2 and 4 weeks. (C) The track visualizations, heatmaps and the discrimination and preference index of 2 weeks NOR test. (D-E) The total exploration time and frequency of familiar or novel objects of 2 weeks NOR test. (F) The track visualizations, heatmaps and the discrimination and preference index of 4 weeks NOR test. (G-H) The total exploration time and frequency of familiar or novel objects of 4 weeks NOR test. Asterisks indicate statistical significance (*p < 0.05; **p < 0.01; ***p < 0.001; ****p < 0.0001). All data are presented as mean ± SEM.

2. Identification of hippocampal cell clusters in mice with chronic METH exposure

To investigate the impact of chronic METH abuse, single-cell RNA-seq was performed on the hippocampi of mice treated with either saline or METH. A total of 60,549 high-quality cells were obtained after stringent quality filtering, including 31,219 cells from saline-treated mice and 29,330 cells from METH-treated mice. Clustering analysis was then conducted based on gene expression profiles using cluster-specific variable genes, following the Seurat pipeline (logfc.threshold = 0.25, min.pct = 0.25). Subsequently, Uniform Manifold Approximation and Projection (UMAP) analysis at a resolution of 0.8 identified a total of 31 distinct transcriptional clusters in each experimental group (Fig.2.A). Using established hippocampal markers from databases (primarily CellMarker2.0 and PanglaoDB), we annotated 18 distinct cell types within the hippocampus. These included astrocytes (cluster 6 and 27, marked by *Aqp4*, *Gfap*, *Gja1*, and *Slc1a3*), Cajal-Retzius cells (cluster 14, marked by *Cntnap2*, *Reln*, *Clstn2*, and *Kcnh7*), Cldn5^{+} and Cldn5^{-} mural cells (cluster 9 and 11, marked by *Vtn*, *Pdgfrb*, *Rgs5*, and *Atp13a5*, distinguished by high or low expression of *Cldn5*), endothelial cells (cluster 4, 7, 8, 10, and 16, marked by *Cldn5*, *Flt1*, *Pecam1*, and *Kdr*), ependymal cells (cluster 23, marked by *Ccdc153*, *Tmem212*, *Rarres2*, and *Mia*), fibroblasts (cluster 25, marked by *Dcn*, *Spp1*, *Nupr1*, and *Igfbp2*), macrophages (cluster 12, marked by *Pf4*, *Mrc1*, *F13a1*, and *Lyz2*), microglia (cluster 0, 1, 3, 21, and 29, marked by *Tmem119*, *Cx3cr1*, *P2ry12*, and *Aif1*), neurons or neuroblasts (cluster 17, marked by *Igfbpl1*, *Sox11*, *Fabp7*, and *Nnat*), neutrophils (cluster 26, marked by *S100a9*, *Retnlg*, *G0s2*, and *Slpi*), NK-T cells (cluster 19, marked by *Ccl5*, *Trbc2*, *Cd3g*, and *Ms4a4b*), neural stem cells (NSCs, cluster 20, marked by *Clu*, *Aldoc*, *Cpe*, and *Hopx*), neurons derived from NSCs (cluster 22, marked by *Chchd10*, *Pcp4*, *Fxyd1*, and *Ppp1r1b*), oligodendrocytes (cluster 2, 5, 24, 28, and 30, marked by *Mbp*, *Mog*, *Cldn11*, and *Mag*; cluster 24 was identified as perivascular oligodendrocytes), oligodendrocyte precursor cells (cluster 13, marked by *Pdgfra*, *Cacng4*, *Sox10*, and *Cspg4*), smooth muscle cells (cluster 15, marked by *Acta2*, *Myl9*, *Tagln*, and *Myh11*), and T cells (cluster 18, marked by *Cd44*, *Cd52*, *Cd74*, and *Plac8*). The top four highly expressed genes for each cluster are displayed (Fig.2.B &D, SI.1). These findings indicate that, in addition to neurons, the hippocampus comprises a diverse array of cell types, including neuroglia, stromal cells, vascular cells, and immune cells, forming a complex yet highly organized microenvironment. Within this microenvironment, METH exerts widespread effects across multiple cell types, potentially contributing to impairments in learning and memory. This knowledge may help elucidate the characteristics and functional alterations of specific hippocampal cell types under chronic METH exposure.

Following clustering analyses, cell proportion analysis revealed that chronic METH exposure led to a decrease in the proportion of astrocytes from 6.6% to 5.5%, endothelial cells from 24.3% to 22.5%, smooth muscle cells from 1.0% to 0.6%, oligodendrocyte precursor cells from 1.6% to 1.0%, neutrophils from 0.3% to 0.1%, ependymal cells from 0.4% to 0.3%, and fibroblasts from 0.3% to 0.2%. Conversely, an increase was observed in the proportion of microglia from 36.0% to 39.8%, NK-T cells from 0.5% to 0.7%, and neurons derived from NSCs from 0.2% to 0.6% (Fig. 2.C).

3. Chronic METH exposure induced gene and function changes of hippocampal cells in mice

Chronic METH abuse elicits a diverse array of cellular responses, ultimately resulting in multifactorial cognitive decline. To elucidate the underlying mechanisms of this cognitive impairment, we employed muscat — a pseudobulk-based analytical framework — for multi-sample, multi-condition, cluster-specific differential gene expression analysis, enabling the identification of differentially expressed genes (DEGs) within each cell cluster. Strikingly, most DEGs were found to be specific to individual cell types following chronic METH exposure. For example, Cldn5^{+} mural cells exhibited the highest number of DEGs, with 679 identified (368 upregulated and 311 downregulated) (Fig.3.A), including 336 cell type-specific DEGs (Fig.3.B).

Fig. 2. Hippocampus cell clusters of saline and METH mice.

(A) The Umap-distributed plots showing 31 hippocampal cell clusters in saline and METH groups. (B) The average expression of known marker genes of hippocampal clusters. (C) The percentage of cells in hippocampal clusters in saline and METH groups. (D) The marker genes expression's featureplots of astrocyte, endothelia, microglia and oligodendrocyte.

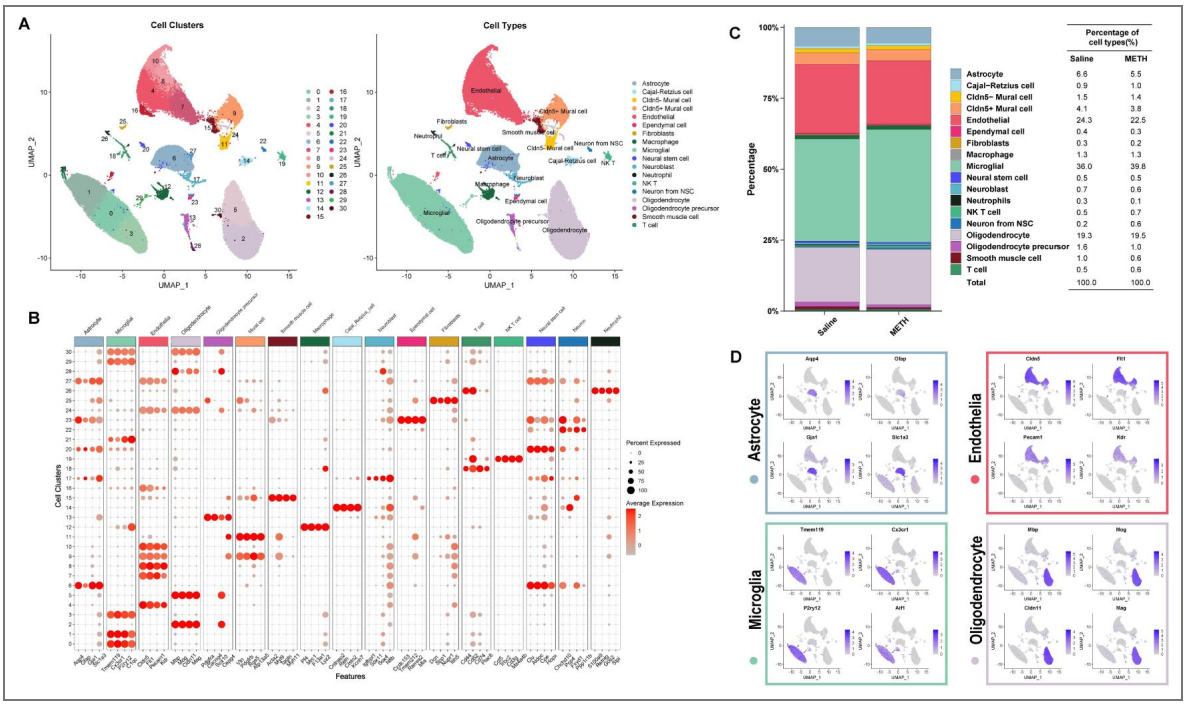

Fig. 3. Differentally expressed genes(DEGs) induced by chronic METH exposure in hippocampal cell types.

(A) The manhattanplot showing the number of DEGs in each hippocampal cell types(METH v.s. saline), the red dots and number represented for up-regulated genes and the blue ones represented for down-regulated genes. (B) The upset plot showing the number of all of unique and some of shared genes of hippocampal cell types. (C-F) The biocprocess in GO terms enriched separately by up or down-regulated genes of astrocyte, endothelia, microglia and oligodendrocyte. Criteria for DEGs by Muscat: p_value < 0.05, abs(log2FC) > 0.25).

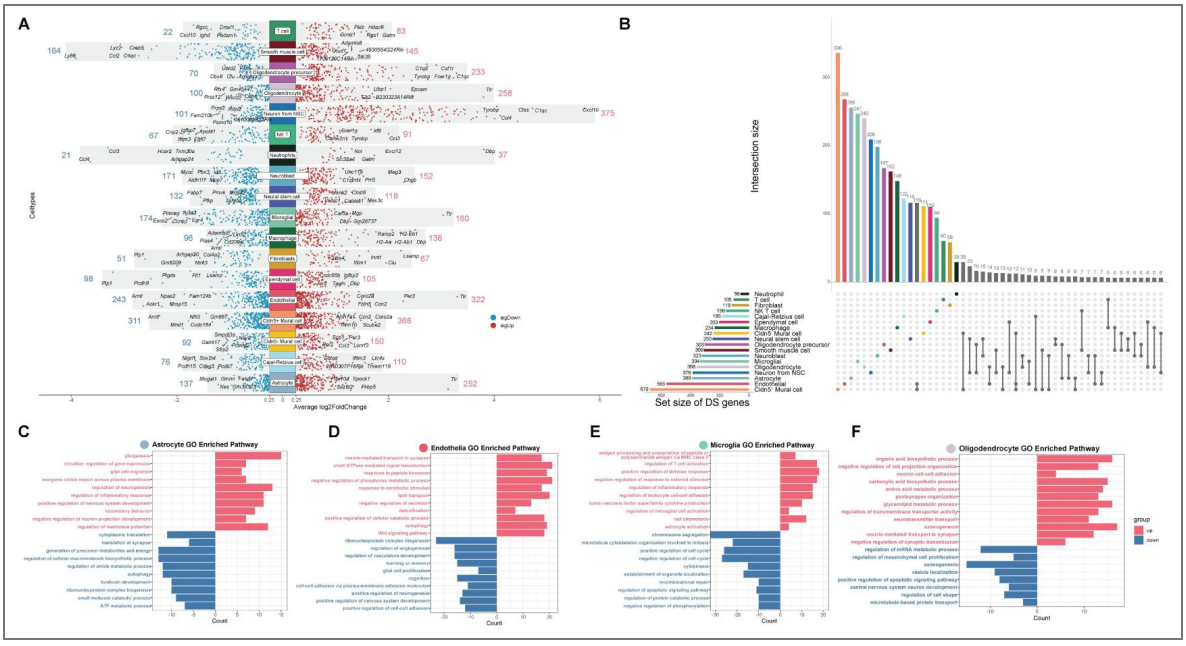

Similarly, endothelial cells showed 565 DEGs (322 upregulated and 243 downregulated) (Fig.3.A), of which 268 were cell type-specific. Notably, a subset of 116 DEGs was shared between these two cell types (Fig.3.B).

These DEGs were subsequently categorized based on their direction of regulation (upregulated or downregulated) and subjected individually to pathway enrichment analysis using Gene Ontology (GO), in order to elucidate their functional roles and the molecular basis of METH-induced cognitive decline. The upregulated and downregulated Biological Processes (BP) from the GO analysis are presented (Fig.3.C – F and SI.2). Moreover, analysis of cell type-specific enrichment patterns revealed that, in addition to distinct functional effects, there exist complex co-regulatory mechanisms across different cell types in response to chronic METH exposure.

Neuroinflammation is a complex process that can be triggered by various factors, such as exposure to toxic substances like METH. METH-induced neuronopathies, in particular, have been found to constantly produce a range of impact factors and cells' changes that contribute to the exacerbation of neuroinflammation. Microglia up regulates immunoprotein receptor genes (such as *Fcer1g*, *Fcgr3* and *Il1rl2*) to enhance immune sigal reception and cell chemotaxis (*Ccl2*, *Cxcl14*, *Trpv4*, et al.) (Fig.3.E). Astrocytes enhance their capacity for gliogenesis and migration through the expression of key regulatory genes (*P2ry12*, *Rras*, *Efemp1*,et al.) thereby modulating the inflammatory response via the NF-κ B signaling pathway (involves *Tnfaip6*, *Nfkb1*,*Nfkbia*) (Fig.3.C). In addition to the responses of neurogliocytes, genes like *Grn* and *Trem2* (associated with astrocye and microglia activation) are up-regrated in both microglia and T cell, suggesting potential communication between central resident and peripheral immune cells, which may jointly participate in the neuroinflammatory response. T and NK-T cells become more active in leukocyte or lymphocyte mediated immunity, but T cells active by complement-mediation (*C1qb*, *C1qc*, *C1qa*, *Trem2*) while NK-T cells depend more on reception of cytokines (*Il18r1*, *Fcer1g*) or recognition of receptors on membrane (*Itgb2*, *Ptprc*, *Tyrobp*,et al.). However neutrophils down-regulate chemokine-mediated signaling pathway (*Cxcr4*, *Ccl3*, *Ccl4*) that may indicates neuroinflammation changes from acute (leukocyte-leading) to chronic (lymphocyte-leading). Macrophage also weaken leukocyte activation (*Cd28*, *Itgam*, *Il18*, *Tnfsf9*, et al.) but strengthen T cell activation.

The maintenance of a stable neural microenvironment relies on a healthy blood-brain barrier (BBB) system(13). METH can induce structure and function disruptions in the BBB, although its chronic effects remain uncertain. In our study, we observe that endothelial cells upregulate detoxification funtions (*Gstm1*, *Abcg2*, *Fbln5*, et al.) and autophagy-related genes (*Qsox1*, *Fnbp1l*, *Trp53inp1*, et al.), while downregulating angiogenesis-associated genes (*Hipk2*, *Tnfrsf1a*, *Vegfc*, *Cldn5*, et al.) and cell-cell adhesion molecules (*Hmcn1*, *Ceacam1*, *Cdh10*, et al.). Furthermore,endothelial dysfunction is also implicated in learning or memory deficits and cognitive impairments (*Dbi*, *Bche*, *Psen2*, *Prnp*, et al.) as well as nervous system development (*Macf1*, *Ptprz1*, *Vegfc*, *Ctnnb1*, et al.) suggesting an interplay between neuronal activities and vascular functions (Fig.3.D). Similarly,dysfunctions in *Cldn5*$^{+}$ mural cells are associated with altered vascular permeability (*Ctnnbip1*, *Pde3a*, *Ceacam1*, *Cldn5*) and developmental processes (*Atp2b4*, *Sfrp2*, *Vegfc*, *Tgfbr2*, et al.), as well as cognitive impairments (*Psen2*, *Bche*, *Nf1*, *Prkn*, et al.), and increased autophagic cell death (*Bmf*, *Bnip3*, *Lamp1*, *Cdkn2d*) after METH trearment. As a structure of arteriole in hippocampus, SMCs exhibit suppressed inflammatory responses such as leukocyte migration (*Abl2*, *Fcer1g*, *Vcam1*, *Icam1*, et al.), glial cell activation (*Syt11*, *C1qa*, *Cx3cr1*, *Trem2*, et al.) and IL-6 production (*Dhx9*, *Fcer1g*, *Syt11*, *Il6ra*).

The response of BBB cell types to METH is heterogeneous(14). In our data, within the Wnt signaling pathway—which promotes angiogenesis and vascular remodeling(15)—both *Cldn5*$^{+}$ and *Cldn5*$^{-}$ mural cells show downregulation through distinct sets of DEGs, whereas endothelial cells exhibit upregulation of this pathway. Cell-substrate adhesion is enhanced in mural cells and SMCs, but reduced in ECs. Although this ultimately results in increased BBB permeability, the underlying mechanisms differ between the inner and outer layers of the vasculature.

Metabolite shuttling and extracellular vesicle signaling provided by oligodendrocytes are essential for the normal functioning of neurons, particularly their axons(16). In our study, we observed significant changes in the metabolic status of oligodendrocytes (Fig.3.F), including alterations in organic acid biosynthesis (*Cyp27a1*, *Per2*, *Glul*, et al.), amino acid metabolic (*Glul*, *Bcat1*, *Hmgcll1*, et al.), glycolipid metabolic process (*Pikfyve*, *Pigc*, *Pnpla7*, et al.) and other processes. Additionally, METH influences neural structure and function-related changes such as axonogenesis (GO terms:axonogenesis, postsynapse organization, central nervous system neuron development, et al.) and synaptic vesicle signaling (GO terms: vesicle-mediated transport in synapse, synaptic vesicle recycling, vesicle localization, et al.), which are partially upregulated or downregulated. Furthermore, oligodendrocyte precursor cells exhibit negative effects on cell development and synaptic plasticity while also increasing neuroinflammation response to DNA damage stimulus. These effects may contribute to neuronal dysfunction and ultimately lead to cognitive decline. Astrocytes play a vital role in supporting neuronal function throughout the central nervous system by regulating synapse development and neurotransmitter release at synapses while providing adequate energy supply and modulating information processing within neurons(17). During chronic METH abuse, astrocytes downregulate bioprocesses involved in translation and metabolism (Fig.3.C), such as translation at synapse (*Rpl12*, *Rpl35*, *Rps26*, et al.) and the generation of precursor metabolites and energy (*Adh5*, *Ndufa5*, *Bpgm*, et al.), which may impede normal neurotransmitter vesicle transmission. Simultaneously, astrocytes enhance bioprocesses related to multiple inorganic cation transportation including potassium (*P2ry12*, *Kcnd3*, *Slc24a2*, et al.), sodium (*Slc24a2*, *Nkain1*, *Hcn2*, et al.), or calcium (*P2ry12*, *Tmem38a*, *Slc24a4*), which may interfere regulation of neural membrane potential. However, we also observe that astrocytes have positive effects of neuron projection extension (*Nrp2*, *Rtn4*, *Jade2*, et al.), axon ensheathment (*Abca2*, *Mal*, *Ugt8a*, et al.), or oligodendrocyte differentiation (*Abca2*, *Mal*, *Mag*, et al.). These results may imply that astroctyes have dfferent subsets performing diverse functions according to their positions and cellular contacts in hippocampus.

Adult hippocampal neurogenesis (AHN) is a complex and dynamic developmental process regulated by a multitude of factors. It involves a sequential progression from neural stem cells (NSCs), through radial glia-like cells and neuroblasts, to fully differentiated mature neurons. This process plays a crucial role in cognitive functions such as learning, memory formation, and emotional regulation. Furthermore, alterations in AHN have been associated with memory impairments, highlighting its significance in maintaining hippocampal plasticity and overall brain function(18). At the initiation of adult hippocampal neurogenesis (AHN), we observe that neural stem cells (NSCs) downregulate pathways related to the generation of precursor metabolites and energy (e.g., *Sdhaf4*, *Nduf* family, *Uqcrh*, *Gapdh*), suggesting that METH may impair the proliferation and differentiation potential of NSCs. Furthermore, METH induces endoplasmic reticulum stress (e.g., *Tmco1*, *Atf3*, *Hspa5*, *Gsk3b*), activates apoptotic processes (e.g., *Btg2*, *Prnp*, *Cebpb*, *Ctsz*), and promotes autophagy (e.g., *Ddrgk1*, *Ctsa*, *Mcl1*, *Sh3glb1*) in NSCs. These alterations consequently lead to increased expression of β-amyloid-related genes (e.g., *Prnp*, *Apoe*, *Psenen*, *Rtn4*) and IL-6-related genes (e.g., *Ncl*, *Fcer1g*, *Il1a*, *Lbp*), which may trigger neuroinflammatory responses. Adult NSC activation in mice is known to be regulated by circadian rhythms and intracellular calcium dynamics(19). In our dataset, astrocytes from METH-treated mice show enhanced expression of circadian rhythm-related genes (e.g., *Per2*, *Ptgds*, *Ciart*, *Id3*), calcium-mediated signaling pathways (as previously mentioned), and genes involved in the regulation of neurogenesis (e.g., *Per2*, *Mag*, *Fbxo31*, *Slc7a5*). These findings suggest that astrocytes may attempt to compensate for METH-induced damage by activating NSCs; however, this compensatory mechanism could accelerate the depletion of the NSC pool.

During the neuroblast stage, METH exposure increases oxidative stress through upregulation of genes associated with oxidative stress response (e.g., *Setx*, *Prkra*, *Agap3*, *Lig1*) and alters DNA regulatory mechanisms involved in cell division (e.g., *Ciz1*, *Rpa2*, *Mcm7*, *Ssbp1*). Additionally, METH suppresses cell-substrate adhesion by downregulating genes such as *Myoc*, *Ccn1*, *Ptn*, and *Lrp1*. As the remaining neuroblasts mature into neurons, METH exerts more pronounced effects, resulting in a higher number of DEGs. Under METH exposure, neurons derived from NSCs upregulate pathways related to endoplasmic reticulum stress (e.g., *Tmco1*, *Atf3*, *Hspa5*, *Pdia3*), TNF

superfamily cytokine production (e.g., *Ncl*, *Fcer1g*, *Il1a*, *Lbp*), neuron death (e.g., *Prnp*, *Ctsz*, *Mcl1*, *Jun*), leukocyte chemotaxis (e.g., *Fcer1g*, *Lbp*, *Cxcl10*, *Hmgb1*), and β-amyloid metabolic processes (e.g., *Prnp*, *Apoe*, *Psenen*, *Rtn4*). Simultaneously, these neurons downregulate key pathways involved in energy metabolism (e.g., *Sdhaf4*, *Nduf* family, *Cycs*, *Gapdh*) and mitochondrial structure and function (e.g., *Slc25a* family, *Vdac1*, *Atpif1*, *Acaa2*).

Cajal-Retzius cells (CRs) are transient neurons that almost completely disappear in the neocortex after birth but survive up to adulthood in the hippocampus at a certain percentage. CRs are synaptically integrated into hippocampal circuits relating to hippocampal-related behaviors and network. Abnormal survival of CRs has been linked to deficits in adult neuronal and cognitive functions(20, 21). In our analysis, CRs down-regulate various neural growth and maturation-relevant processes including axon extension (e.g.,*Sema6d*, *Dclk1*, *Cttn*, *Sin3a*), dendrite genesis (e.g., *Nlgn1*, *Dclk1*, *Farp1*, *Il1rapl1*), synapse organization (e.g., Lrrtm4, Lhfpl4, Farp1, Mark2) and neuron migration (e.g., *Nr4a2*, *Dclk1*, *Sema6a*, *Mark2*, *Cdkl5*).

In summary, METH exerts direct neurotoxic effects on NSCs and their developmental trajectory, while also indirectly disrupting the function of neurogenesis-supporting cells, ultimately contributing to cognitive decline.

Ependymal cells, a type of neuroglia that provides support to neurons, form the epithelial lining of the brain ventricles(22). METH exposure induces significant changes in ependymal cells, including the upregulation of genes associated with cilium organization and motility (e.g.,*Meig1*, *Cfap* family, *Lca5*, *Tmem216*), suggesting enhanced cerebrospinal fluid circulation and a potential compensatory response to toxic substances by facilitating the clearance of harmful molecules. However, METH also downregulates genes involved in intracellular transport (e.g., *Ptpn14*, *Pdcd10*, *Txn1*, *Sorl1*) and protein processing (e.g., *Gsn*, *Txn1*, *Tmsb10*, *Sorl1*), indicating impaired cellular functions that may compromise ependymal cell homeostasis.

Fibroblasts, which originate from embryonic mesenchymal cells, perform a variety of complex and diverse functions in the hippocampus, including extracellular matrix (ECM) homeostasis, secretome regulation, mechanosensation, progenitor cell activity, and immune modulation(23). However, their specific roles in this brain region remain incompletely understood. Compared to the saline group, METH-treated fibroblasts exhibit increased expression of genes associated with responses to metal ions (e.g., *Gsn*, *Mt2*, *Mt1*, *Id2*, *Hnrnpa1*) and toxic substances (e.g., *Gstm1*, *Inmt*, *Mt2*, *Mt1*), as well as markers linked to astrocyte differentiation (e.g., *Vim*, *Plpp3*, *Sox9*, *Id2*). Notably, downregulation of the JNK and MAPK signaling pathways (e.g., *Map4k4*, *Sh3rf1*, *Ccn2*, *Gadd45b*, *Dab2*) is associated with reduced fibrosis, suggesting that fibroblasts may undergo functional transitions— from stress responses such as cell death and inflammation—to roles in cellular support and transformation.

4. METH-induced alterations of crosstalk between cell types in hippocampus led to hippocampal environment disturbance

Considering the neurotoxic effects of METH on various cell types in the hippocampus and its intricate impact, we conducted an investigation into hippocampal intercellular communication to elucidate the role of these interactions in cognitive decline. Our findings reveal a slight increase in both the total number of cell communication interactions (from 18,396 to 19,054) and their strength (from 0.883 to 0.841) following METH treatment (Fig.4.A). The results demonstrate that chronic METH abuse induces a greater diversity of changes in the differential number of interactions among cell types compared to changes in interaction strength (Fig.4.B and C). For instance, astrocytes mildly enhance the number of interactions with mural cells, ECs, and OPCs but decrease the strength of these interactions, suggesting reduced efficacy of communication signals under METH influence. Neuron derived from NSCs increase the number of interactions with most cell types while exhibiting minimal changes in interaction strength, which corresponds to the up-regulation of TNF superfamily cytokines and damage signals associated with ER stress or amyloid-

beta mentioned in DEGs analysis. In association with neuroinflammatory response, microglia significantly augment their own interaction strength, potentially contributing to neuroinflammation.

From the perspective of cellular communication patterns (incoming and outgoing), hippocampal cells treated with METH exhibit 4 incoming patterns similar to the Saline groups, primarily related to microglial activation, BBB function, neural development, and immunity (Fig.4.D). However, in terms of outgoing patterns, the communication patterns of METH groups are divided into 8 distinct patterns compared to 5 in the Saline group. These outcoming patterns mainly involve microglia activation, endothelial cell signaling, neural development processes, immune responses, as well as a mixed pattern reflecting changes in the neural microenvironment (Fig.4.E). The disruption caused by METH results in confusion within cellular crosstalk specifically through disturbances in outcoming communication pathways within the hippocampus. To further elucidate how METH affects cellular communication networks concretely, we conducted an analysis focusing on specific signal pathway alterations. By calculating Euclidean distance (Fig.4.F), we identified several key differential functions between METH and Saline groups: RANKL (Receptor Activator of Nuclear Factor-κ B Ligand, belongs to tumor necrosis factor (ligand) superfamily, also proteinically known as TNF-related activation-induced cytokine), SELPLG (proteinically known as p-selectin, involving in leukocyte and microglia activation(24)), and CD46 (proteinically known as complement regulatory protein, as a membrane cofactor mediated cleavage cofactor of C3b and C4b, which is a key regulator of classical and selective complement activation cascade, as well as inflammation(25)). We then compared overall information flow across each signal path to determine conservative and METH-specific signaling pathways (Fig.4.G). Additionally, we also examined changes occurring within each outgoing or incoming signal pathway for individual cell types (Fig.4.H).

5. Pseudo-time series analysis revealed that METH caused changes in hippocampal neurogenesis in mice

Adult neurogenesis in the dentate gyrus of the hippocampus plays a crucial role in cognitive function in mice and is influenced by the local microenvironment or niche(26). However, limited evidence exists regarding the impact of METH exposure on the capacity of NSCs to differentiate into neurons, astrocytes, oligodendrocytes, and other cell types. To address this, we conducted pseudotime analysis to explore how chronic METH exposure affects NSC differentiation trajectories.

Along the temporal axis, with NSCs as the starting point, we observed that under normal conditions (Saline group), NSCs (cluster 20) predominantly differentiated into neuroblasts (cluster 17) compared to astrocytes (clusters 6 and 27), following a typical neural developmental trajectory (Fig.5.A). In contrast, METH exposure disrupted this pattern, showing an increased tendency for NSCs to differentiate into astrocytes rather than neuroblasts (Fig.5.D), suggesting impaired neurogenesis.

Our analysis reveals that the altered neural developmental trajectory in the METH group is associated with changes in the expression of genes such as Bsg, Ccl4, Fos, and Sox11 (Fig.5.F), as illustrated by other differentially expressed genes in the heatmap (Fig.5.E). In contrast, normal developmental progression from NSCs to neuroblasts is more closely associated with the expression of Flt1, Hspb1, Igfbp7, Tmsb10, and other related genes (Fig.5.B and C).

6. The change of transcription factor regulatory network is also the cause of cognitive decline caused by METH

We conducted an analysis of the differential expression of transcription factors in each cell type between METH and Saline mice (Fig.6.A and B). Subsequently, we constructed networks of transcription factor-target genes to predict changes in cellular functions (Fig.6.D-H, SI.3).

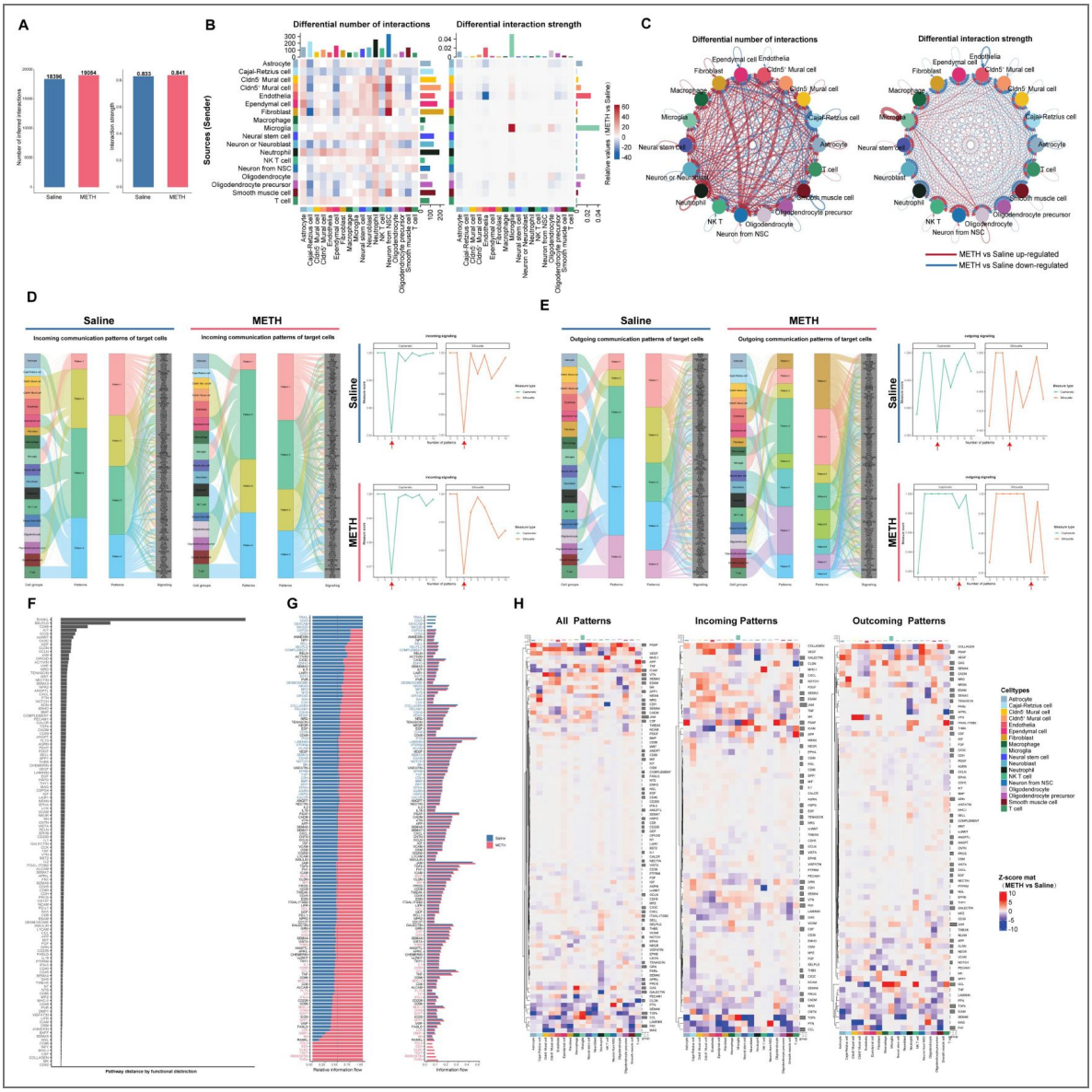

Fig. 4. Hippocampal cell types crosstalk alterations induced by chronic METH treatment.

(A) The total number of cell communication interactions and the intensity of interactions in saline and METH groups. (B-C) The comparison of the number and the strength of interactions of each cell types between METH and saline groups. (D-E) The incoming and outgoing communication patterns of secreting cells of each groups and the inflection point parameter in clustering algorithm. (F) The identificaton of signaling networks with large (or small) differences according to the Euclidean distance in a shared two-dimensional space. (G) The comparison of the overall information flow of each signal path between two groups. (H) Heatmap showing the incoming, outgoing and all communicated informations' comparison of each signal of each cell type.

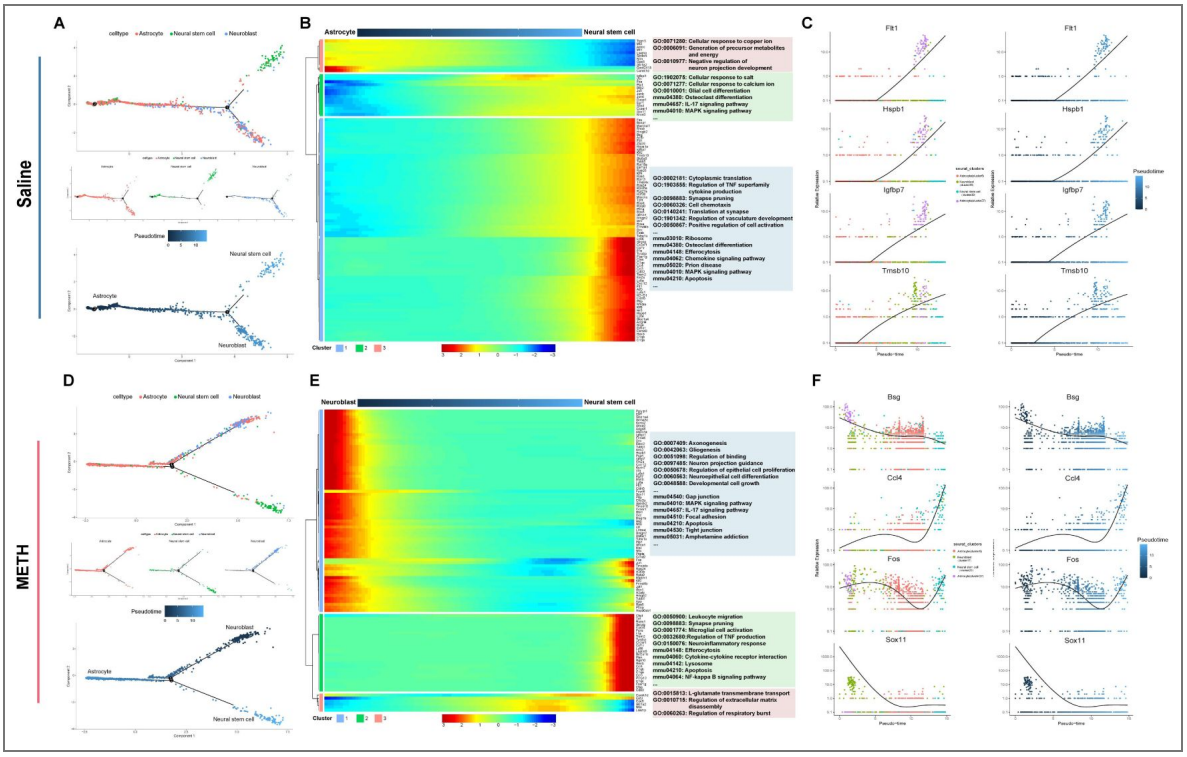

Fig. 5. The development direction of hippocampal neural stem cells and the regeneration of hippocampal nerve were analyzed in pseudo-time series.

(A, C) The pseudo temporal differentiation locus of neural stem cells, astrocytes and neuroblasts in saline (A) or METH (C) group. (B, D) Heatmap showing the expression of specific genes(rows) in subclusters (columns) along the maturation trajectory from neural stem cells to neuroblasts or astrocytes in saline (B) or METH (D) group, and GO or KEGG funtional enrichment of those genes. (E, F) Pseudotime expression graphs of 4 representative specific marker genes in these cell types showing the development tendency difference in saline (E) or METH (F) group.

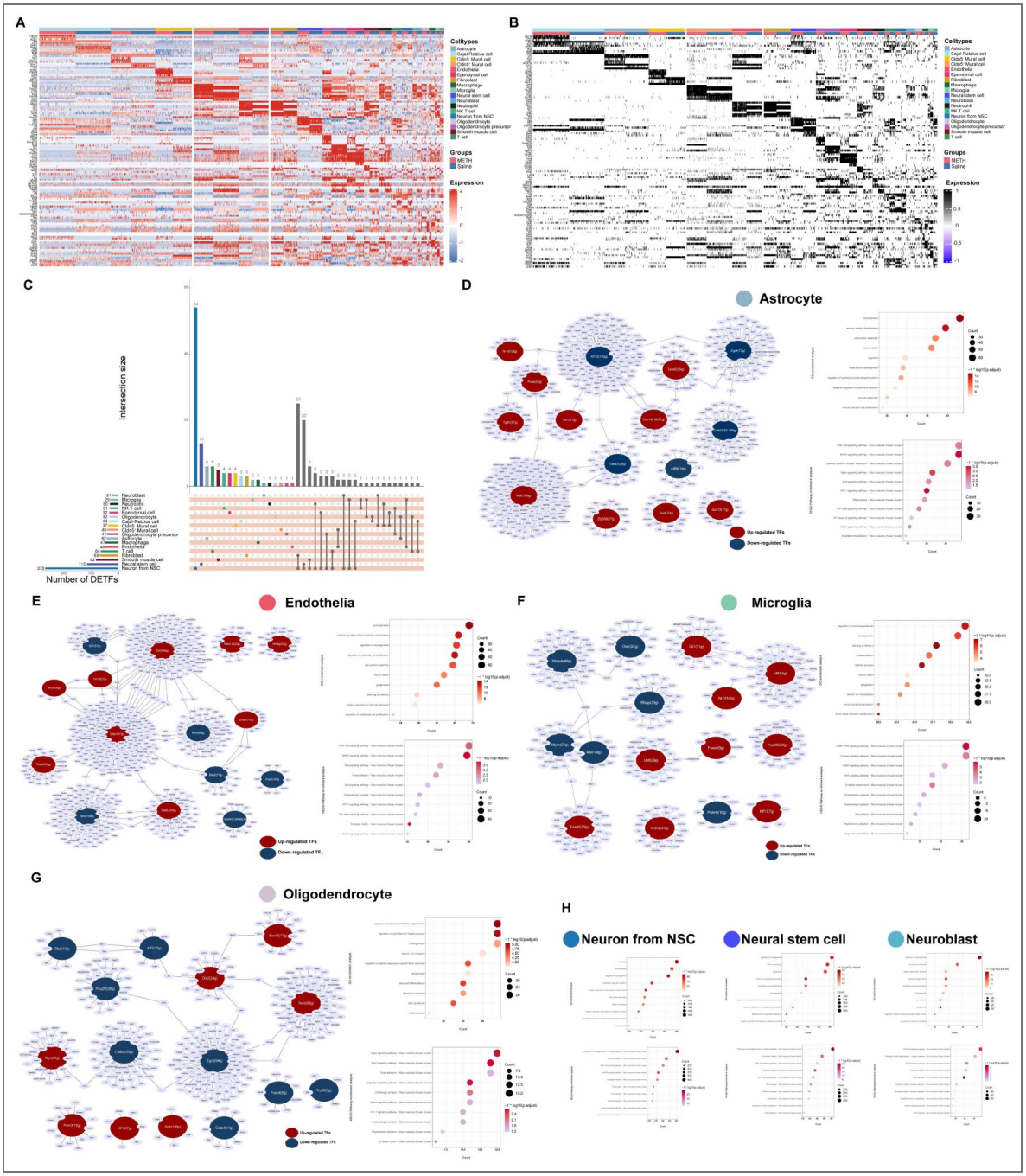

Fig. 6. Transcription factor (TF) analysis and function prediction.

(A-B) Heatmap of the average expression and the area under the curve scores of TF motifs estimated per cell by SCENIC. Shown are top five differentially activated motifs in each cell type of saline and METH groups, respectively. (C) The upset plot showing the number of all of unique and some of shared TFs of hippocampal cell types. (D-G) Gene regulatory network analysis and function enrichment using top 10 of SCENIC identifies critical TFs of astrocytes, endothelia, microglia and oligodendrocytes. (H) Enrichment analysis of target genes predicted by TFs of neuronal development related cell types (Neuron from NSC, NSC and neuroblast).

In astrocytes, a total of 42 differentially expressed transcription factors (DETFs) were identified (Fig.6.C), and their associated target genes were enriched in biological processes related to neurogenesis and development, cognitive function, regulation of inflammatory responses, as well as signaling pathways including PI3K-Akt, MAPK, and cytokine-cytokine receptor interactions, among others (Fig.6.D).

Similarly, endothelial cells exhibited 48 DETFs, whose target genes were also enriched in biological processes related to neural development, including axonogenesis, neuronal differentiation, and functions associated with learning and memory. Endothelial cells share common signaling pathways with astrocytes, such as PI3K-Akt and MAPK (Fig.6.E). Furthermore, biological processes specifically associated with endothelial cells, such as endothelial cell proliferation, cell-cell adhesion, and cell junction assembly, were found to be involved in signaling pathways including Ras, focal adhesion, and Wnt, among others.

Although only 29 DETFs were identified in microglia, they play a significant regulatory role in processes such as membrane potential modulation, axonogenesis, and neuronal death. These biological processes are closely associated with synaptic pruning and neuronal survival, which may ultimately contribute to cognitive dysfunction. Signaling pathways including calcium, Wnt, cGMP, and cAMP are actively involved in the aforementioned processes (Fig.6.F).

As key supporters of neuronal bodies and axons, oligodendrocytes exhibit 32 DETFs that regulate processes related to cytoskeletal fiber organization and axon development. This suggests that METH exposure disrupts the transcriptional regulation of genes involved in neural support, thereby increasing neuronal vulnerability to damage. These effects may be mediated through signaling pathways such as Hippo, FoxO, Apelin, and Focal Adhesion. Whether the transcriptional disruption affects neuronal growth itself or the maintenance of surrounding cells and the neural environment under chronic METH treatment remains an important factor contributing to cognitive decline in mice.

Interestingly, neurons derived from NSCs exhibit the highest and second-highest numbers of DETFs, respectively, and share highly similar functional enrichment terms among their target genes. These terms are primarily associated with neurodegenerative processes such as autophagy and neuronal death, axonogenesis, ameboid cell migration, and biosynthetic activities, which are also comparable to those observed in neuroblasts (Fig.6.H). This indicates that METH may exert common neurotoxic mechanisms in both mature neurons and neural precursor cells by modulating similar pathways through the expression of differentially regulated neural transcription factors.

Discussion

As a psychostimulant drug widely use in worldwide, METH can elevate the risk to various neurological neuropsychiatric disorders due to its addictive and neurotoxic effect. In our study, animal behavior experiments illustrate that chronic METH abuse can cause cognitive decline in mice, which is manifested in spatial cognition, working memory and new object learning. Although previous studies also have similar concusions of METH-induced learning and memory impairments and put forward a variety of therapeutic improvement schemes (e.g. melatonin, oxytocin, housing and tetrahydropalmatine)(27–30), it seems that there are few practical, effective, and recognized treatments for chronic METH abuse-induced cognitive dysfunction therapy. Because researchers have found that METH can affect many organs throughout the body including most areas of the brain by complex and diverse molecular mechanisms, mainly involving excitatory toxicity, neurotransmitter disruption, oxidative stress, cytotoxicity (apoptosis, necrosis, and autophagy), inflammatory response, metabolism disorder et al(31–33). Furthermore, unlike acute METH-induced injury, chronic METH abuse represents a more complex process characterized by concurrent neurotoxic damage and reparative responses(34–36).

The hippocampus plays an essential role in a range of advanced brain functions, including memory and emotional regulation, and spatial navigation, and its impairment or dysfunction have been proved to closely associate with neuropsychological diseases like neurodegeneration,

affective disturbance, and learning disabilities(37).

On the base of our animal behavior results, we used scRNA-seq to investigate all mouse hippocampal cell types except for mature neurons and to explain the heterogeneity of METH effects between different types of cells and provide more targeted mechanisms for METH-induced neurotoxicity and targets for precise therapy. Given that this study aims to capture the complete mRNA expression profile of intact cells, we employed scRNA-seq technology. In contrast to single-cell nucleus sequencing (snRNA-seq), this approach necessitates that cells be maintained under conditions as close to physiological states as possible, thereby requiring high structural integrity, robust viability, and minimal exposure to external perturbations. Accordingly, during sample collection and the preparation of single-cell suspensions, we processed the tissues as rapidly and gently as feasible. Nevertheless, mature neurons — due to their highly differentiated state, limited deformability, and the presence of long axons — are particularly susceptible to damage or functional inactivation during the dissociation process, and are therefore frequently excluded prior to sequencing. Therefore, we propose that the neurons captured in this study predominantly represent immature neurons or a distinct subpopulation of neurons with relatively smaller cell bodies. Although we did not detect the expression profiles of mature neuronal genes, our dataset provides a comprehensive and detailed characterization of various non-neuronal cell types. Each analyzed cell contains the complete mRNA expression profile, which accurately reflects its functional state. Accumulating evidence indicates that non-neuronal cell populations in the brain play a critical role in chronic neurodegenerative diseases, with their functional statessignificantly influencing neuronal activity and serving as potential early biomarkers, contributors to disease pathogenesis, and therapeutic targets(38, 39). Notably, the cognitive impairments induced by chronic METH exposure exhibit certain pathological similarities to those observed in Alzheimer's disease and Parkinson's disease(40, 41). Our dataset offers valuable insights into the functional alterations, predictive dynamics, and intercellular communication of non-neuronal cells following chronic METH exposure, thereby providing robust biological information to enhance our understanding of METH-induced neurotoxicity and cognitive dysfunction.

1. Revealing a novel pattern of neuronal death and elucidating the impact of neuronal interactions with other cells during development and maturation

METH can cause abnormal neuronal function in various direct or indirect ways. METH has a direct toxic effect on neurons causing neuronal damage by various programmed cell death, such as apoptosis, autophagy, necroptosis, pyroptosis, and ferroptosis(42). In spite of mature neurons loss during dissociation, we still isolated the neurons remaining a few NSC markers in some degrees and we considered these neurons developed from NSCs on account of that adult hippocampal neurogenesis is a continuous process. Consistent with previous results, we found a few genes of these neurons related to multiple neuron death biological processes exist differences. For example, Cebpb mediate endoplasmic reticulum stress by Nupr1-C/EBP homologous protein (CHOP) pathway, Prnp/Psenen/apoe are associated with neurodegeneration disease in amyloid-beta metabolic process, Gsk3b increases phosphorylation of Tau, Ddrgk1/Mcl1/Sh3glb1 play important role in mitochondrial autophagy, ATF3 forms dimer with c-Jun to promote apoptosis(43). We also noticed TNF superfamily cytokines and ILs overexpression in these neurons may attracts microglia or actives astrocytes leading to neuron death. Abnormal neuronal function is also indirectly related to METH's effects on various auxiliary cells. Our cellchat data showed these neurons generating more communication signals to vascular cells, fibroblasts and ependymal cells after chronice METH treatment. As sources, these neurons upregulate signals like Vegf (Vascular endothelial growth factor, promoting blood vessel growth and increasing permeability.), Sema3b and Sema3c(are critical for neuron projection, guidance of axons, dendritic spine pruning and ECs repulsion(44–46)), Ptn and Mdk (Pleiotrophin and Midkine, as neurotrophic factors, is critical in different steps of differentiation of different cells both in development and in wound repair, especially in neural regeneration, and is up-regulated in drug abuser and neurodegenerative diseases patient(47).), Igf2 (Insulin-like growth factor 2, emerged as a critical

molecule of synaptic plasticity and learning and memory(48).), and Cxcl12 (concerning about regulating generation, positioning and maturation of new neurons(49, 50), as well as the communication with blood vessels(51).), but downregulate signals like Bmp6 (Bmp6 level shows an increase in AD-related neurogenic deficits(52), and critical functions to EC differentiation(53).), Bmp7 (Bmp7 expression in radial glial cells may promotes neurogenesis, inhibits gliogenesis(54).), and Fgf2 (a crucial molecule modulating cell proliferation and survival in central nervous system(55).). As receptors, there neurons recept signals from vascular cells mainly about extracellular matrix, such as Col (collagen) families and Lam (laminin) families. Our analysis showed METH impedes the neuronal maturation process which closely relied on the regulation of vascular cells (Fig.7).

2. Analysis of dynamic changes in neurogenesis to track spatiotemporal shifts in cell composition, signaling, and functional integration during nervous system development and regeneration

METH can cause damage to neurons through various mechanisms, while also have impacts on neural stem/progenitor cells. However, these impacts seem to be different between researches of actue or chronic abuse, intermittent or continuous administration, addiction or withdrawal(56–59). In the researche of chronic METH abuse, it has reported that METH mainly has negetive effects on stem/progenitor cells resulting decreasement proliferative and neurogenesis capacity(56, 60), and even cell death(61, 62). Here our analysis provided in vivo evidences of neurogenesis alterations under chronice METH abuse. We confirmed METH's neurotoxicity to NSCs and progenitor cells like neuroblasts and CRs, and ulteriorly we used pseudotime to explore its influences on differentiation process and dynamics of neural stem cells. The variations of characteristic genes on each branches of neural development trajectory may reveal inflection points in the direction alterations of NSC development under METH effect. It is also necessary to emphsize accurate quantifications of various types of cells counting in the neurogenetic locus will be helpful to lucubrate the toxicity of METH on neurogenesis (Fig.8).

3. Establish a comprehensive cellular interaction map of the neurovascular unit

BBB injury is one of neurotoxic mechanisms of METH neurotoxicity, however, the impact of METH on BBB and its consequent effects on neural function far exceed the barrier dysfunction and abnormal substance transport mentioned in current researches. Previous studies of METH neurovascular toxicity have reported that ECs structure and function disorder and astrocytes-released cytokines or damage factors induced injury are parts of proper mechanisms for BBB injury(14), however these studies usually consider a single aspect of cell type or mechanism within BBB while current researches emphasize that neurovascular unit (NVU) comprises more informations about microcirculation integrity, vascular function and cellular cooperation, which are important to cognition regulation(63). In our study, we parsed most of NVU components which are consisted of ECs, mural cells, SMCs, gial cells (astrocytes, oligodendrocytes and microglia), neurons and basal matrix. We found that ECs can be grouped into several subsets may related to the difference between arteries and veins and the grade of vascular branches, which make it possible to anaylze endothelial dysfunctions like insufficient nutrient and oxygen transport, low clearance efficiency of metabolic waste in cerebral circulation, or leukocyte adhesion and migration. Moreover, mounting evidences correlate mechanical stress with endothelial function, such as barrier function, inflammatory signaling, apoptosis, oxidative stress, endothelial mesenchymal transformation and aging(64), which means ECs located in different fluid states of vascular segments may be regulated variously as results of METH-induced cerebral blood flow abnormalities(65–67). In the meanwhile, the influence of the endothelium on other cell types is extensive, including but not limited to vascular tone or structure, maintenance of collateral vessels, neurotransmission and neurogenesis(63), as our DEGs analysis found that the effects of METH on ECs are not only to damage the junction structure and cause autophagy apoptosis, but

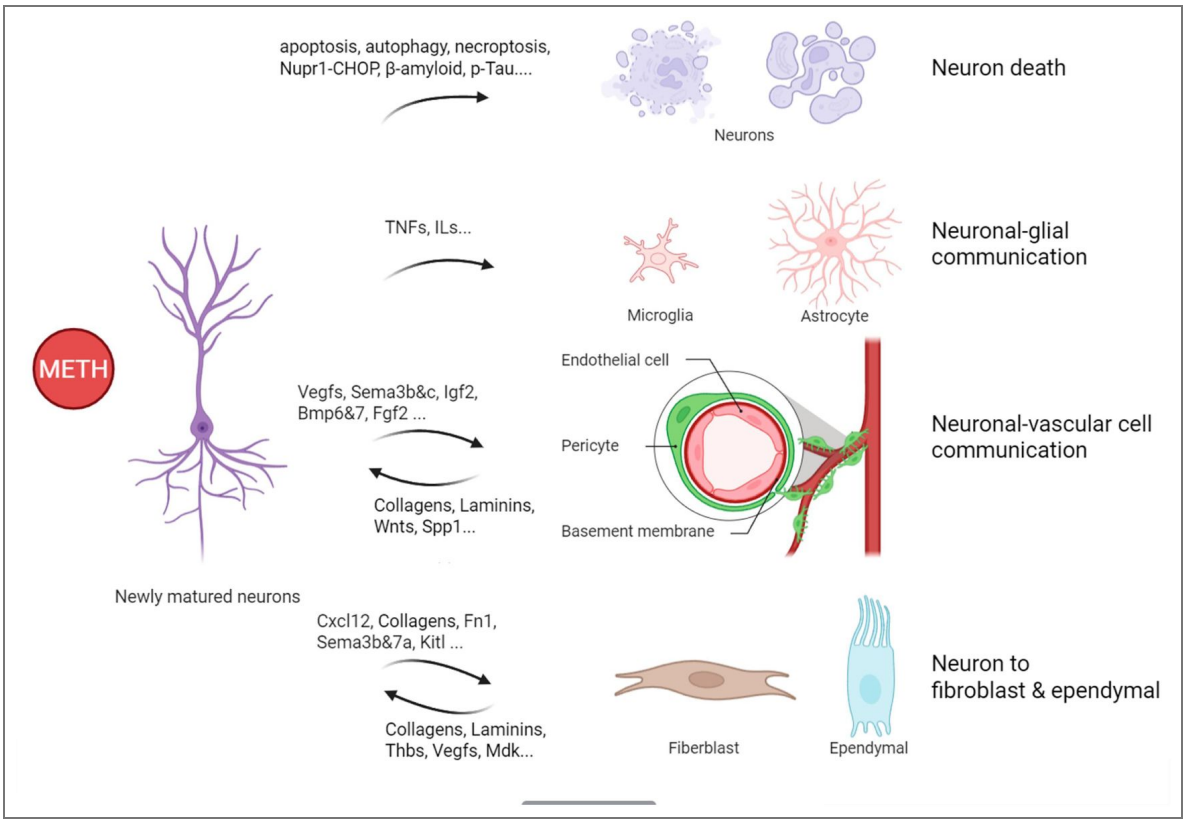

Fig. 7. A schematic illustration of the effects of METH on neuronal cell death during development and maturation and its interactions with glias, vascular cells, fiberblast and ependymal.

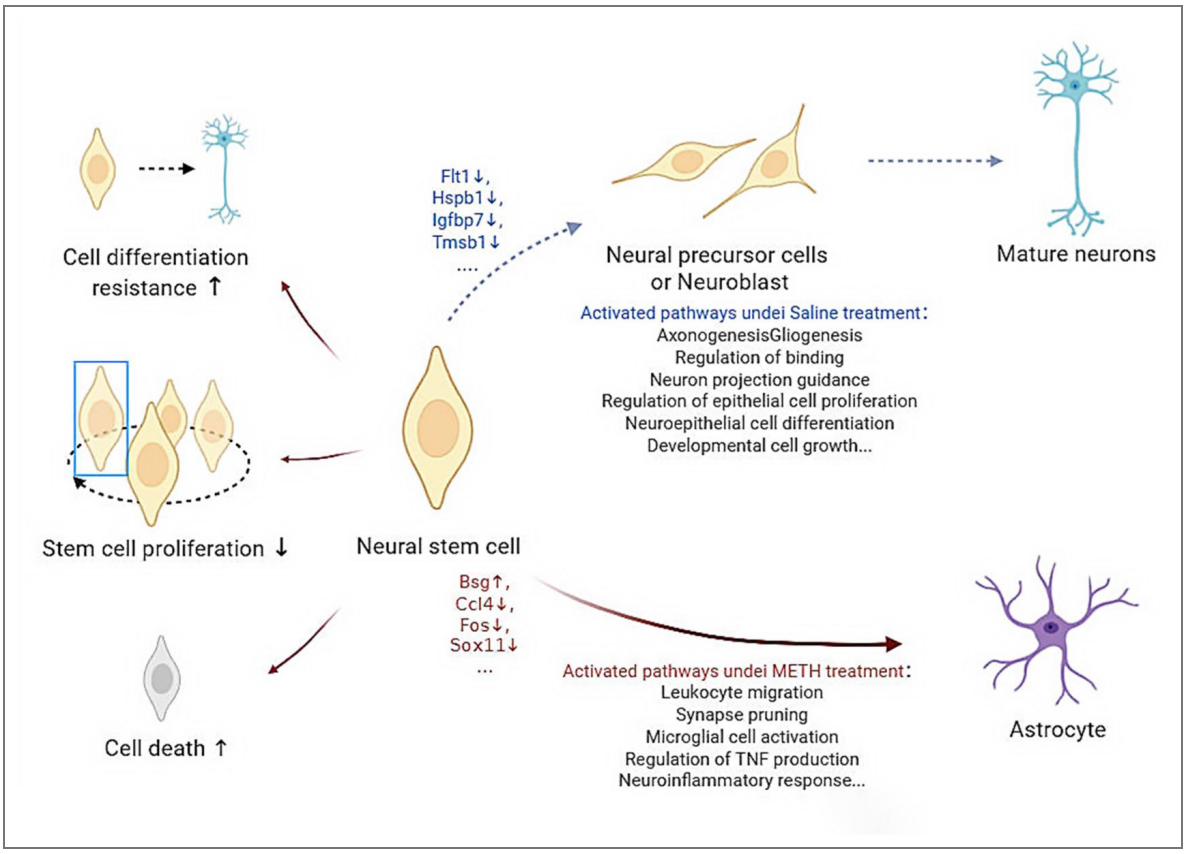

Fig. 8. A schematic illustration of the effects of METH on cell proliferation capacity and cellular activity in neural stem cells, as well as associated alterations in gene expression and signaling pathways during their differentiation into neurons or astrocytes.

also to change the association with other cells, such as GO terms: vesicle-mediated transport in synapse, neurotransmitter transport, or glial cell proliferation. Although there are few METH-induced neurovascular toxicity researches concerning mural cells, who are thought to include pericytes, SMCs and fibroblasts(68), we tried to distinguish them by expression levels of maker genes and eliminate the effect of doublets, and we interestingly found that they share many common genic features as ECs and SMCs, of which some of mural cells have similar expression levels of marker genes as ECs especially. As a result, we classified mural cells as *Cldn5*$^{+}$ and *Cldn5*$^{-}$ mural cells by the similarity to ECs, and we assumed that the diversity of mural cell's functions depends on their proximity and interaction degree to other vascular cells, which is reflecting cellular collaboration in NVU.

4. Chronic METH exposure triggers neuroinflammation through coordinated interactions among immune cells in the central nervous system and peripheral compartments

Traditional METH research has always linked neuroinflammation to astrocytes, microglia, or certain neuroinflammatory factors, but in recent years, the functions of immune cells residing in neural tissue and the neural immune system deserve our attention. Different neural inflammatory factors or immune signals drive different cellular responses through various signaling pathways. As specialized immune cells of the central nervous system, microglia dominate neuroinflammatory processes under chronice METH exposure and play roles as initiators and executors. We found that microglia in our model up-regulates immune and inflammatory responses, such as MHC class II reaction, IL-1 / IL-2 / IL-6 / TNF superfamily cytokines production, and we also noticed that microglia strengthen communications with astrocytes, leukocytes, and lymphocytes whose bioprocesses include activation, differentiation, chemotaxis and migration. It has provided that TNF-α, IL-1α and C1q released by microglia can induce astrocytes to transform into neurotoxic phenotype cells(69). Recent researches pay more attention to the interaction of central and peripheral immune cells influencing neurodegenerations by various mechanisms. Xiaoying Chen et al. reported activate microglia encoding more MHC Ⅰ and Ⅱ proteins recruit T cells into brain parenchyma resulting encephalanalosis(70). Besides, by these innate immune factors, microglia can react to METH-induced DAMPs (Damage Associated Molecular Patterns) from neurons or other cells. We also noticed that some of characteristic cellchat signals induced by METH (such as TIGIT, RANKL, SN, SPP1) are mainly caused by these peripheral immune cells espcially NK-T cells. Astrocytes reshape their morphological, genomic, metabolic, and functional characteristics in response to acute or chronic pathological stimuli through a process called reactive astrogliosis(71). Althought we found astrocytes as a whole can regulate inflammatory response, their functions of different subgroups still need to be classfied by genomic and functional features related to their location and interactions with other cells in the CNS. Specially, we noticed second-messenger-mediated signaling-cAMP is up-regulated in astrocytes, and it may act as a molecular switch for neuroprotective astrocyte reactivity(72). A variety of cells and factors in hippucampal microenvironment participate in or influence neuroinflammation after METH exprosure, our data broadened the research field of neuroinflammation and provided valuable reference genes for various potential inflammatory participants (Fig.9).

5. Identification of disrupted metabolic and circadian coordination across diverse cell types

The metabolism of various cells effected by METH in the hippocampus can not be ignored, as this may also be the cause or result of changes in cell functions. We have paid particular attention to changes in the metabolism of oligodendrocytes, as it is closely related to the support of neural function and structure.we have found that metabolic processes such as the production of organic acids, amino acids, glycerolipids, and glycolipids occur in oligodendrocytes and are similar to the changes in the expression of lipid transport genes emphasized in AD, which may lead to disruptions in myelin formation or energy supply to neurons(73). Furthermore, endothelial cells

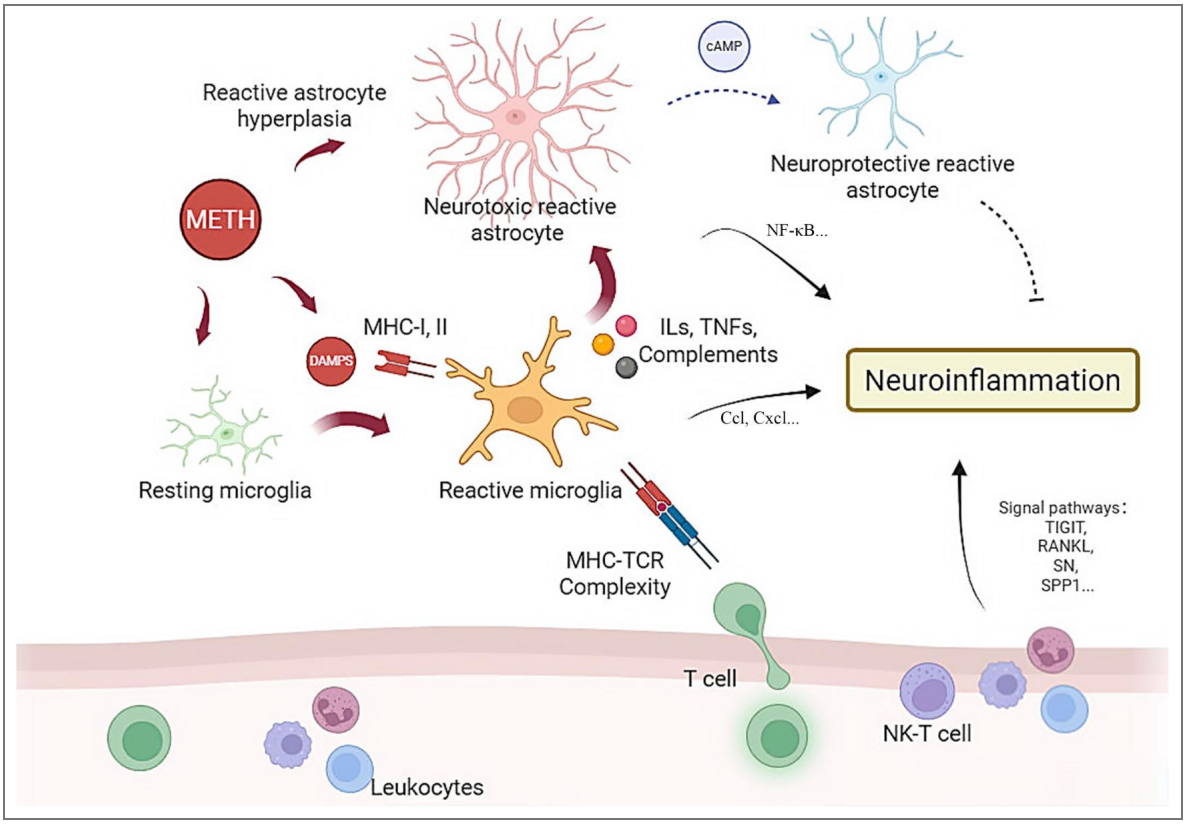

Fig. 9. A schematic illustration of the mechanisms underlying neuroinflammation induced by chronic METH exposure.

METH induces the reactive activation of microglia and astrocytes via multiple signaling pathways and facilitates the recruitment of peripheral lymphocytes and leukocytes to the central nervous system, thereby contributing to the complex regulatory mechanisms underlying the neuroinflammatory response.

and Cldn5^{+} enterocytes both showed impairments in lipid transport, localization, and metabolism, involving genes such as *Slc2a1*, *Mfsd2a*, *Spp1*, *Apoe*, the *Atp* family, and the *Abca* family. While current research suggests that the characteristics of the BBB in a healthy state are not dependent on the maintenance of microglial cells, the microglial scavenger PLX5622 has been found to impact endothelial cholesterol metabolism(74). Additionally, impaired lipid metabolism in microglial cells is considered an important pathogenic factor in AD(75). So we hypothesize that endothelial and epithelial cell lipid metabolism and transport disorders triggered by METH may promote lipid accumulation in microglia and cause neurological damage.

The disruption of circadian rhythms has rarely been mentioned in previous studies on METH, but METH, as a neurostimulant drug often used in nightlife, can affect sleep. Interestingly, the frequent occurrence of circadian regulation in our analysis of a number of cell-types is also worthy of attention, e.g. Genes involved in circadian rhythm regulation, like *Per2*, *Per3, Ciart*, *Nr1d1* or *Nr1d2*, are up-regulated in gliocytes such as astrocytes, oligodendrocytes and microglia, *Nrd1*, *Nrd2*, *Sfpq* (regulates the circadian clock by repressing the transcriptional activator activity of the CLOCK-ARNTL heterodimer(76)) are up-regulated in macrophage. Recent research had reported that the circadian clock regulates the immune response of various peripheral innate and adaptive immune cell types and astrocytes and microglia also possess functioning circadian clocks, and circadian timing can affect their inflammatory response, which may be the regulatory mechanism of neuroinflammation in AD(77). Moreover, we noticed that circadian rhythm disorder in endothelia (involving *Per2*, *Cry2*, *Cry1* and *Ptger4*) , smooth muscle cells (involving *Cavin3*, *Kmt2a*, *Per1*, *Nr1d2* et al.) and ependymal cells (involving *Phlpp1*, *Ptgds*, *Clock*, *Id2*). Existing researches showed that the clearance of metabolites, transporter function, permeability, vascular inflammatory and vasomotion of BBB are regulated by circadian rhythm(78–80). A few studies of METH abuse were concerned about circadian rhythm disorder and reported that METH-associated heart failure(81), variability of body temperature(82), Learned motivation(83), addictive properties(84) and learning and memory impairments(28) are affected by disrupted circadian rhythms. However it still needs more researches to figure out the mechanisms of circadian rhythm disturbed by METH and how does circadian rhythm disruption cause METH toxicity.

Conclusion

In conclusion, our reaserch provides scRNA data on the changes of various types of cells in the hippocampus of mice with cognitive impairment caused by METH exposure. These results provide new insights while partially confirming the results of previous studies on METH neurotoxicity. And we will conduct more confirmatory work in the future to elucidate the mechanisms of neurotoxicity and cognitive decline caused by chronic METH abuse.

Data availability

The single-cell RNA-seq data that support findings of this study are available in Gene Expression Omnibus (GEO) under accession numbers GSE252939. All data generated or analyzed during this study are included in the manuscript and supporting files

Additional information

Ethics approval and consent to participate

All protocols approved by the Institutional Animal Care and Use Committee in Southern Medical University (Ethical number: L2022125), and consistent with NIH Guidelines for the Care and Use of Laboratory Animals (8th Edition, U.S. National Research Council, 2011).

Consent for publication

All authors have approved the manuscript and this submission.

Funding

This work was supported by the Research Projects of National Natural Science Foundation of China (No.82271930) and GuangDong Basic and Applied Basic Research Foundation (2024A1515013050, 2021A1515010909 and 2022A1515110743). The research platforms were supported by Southern Medical University (SMU), Institute of forensic medicine of SMU. We thank Seekgene Biotechnology Co., Ltd for helpful technical support.

Authors and Affiliations

School of Forensic Medicine, Southern Medical University, Guangzhou 510515, Guangdong province, People' s Republicof China: DF Qiao, H Qiu, X Yue, YB Huang, ZL Meng.

Cancer Research Institute, School of Basic Medical Sciences, Southern Medical University, Guangzhou 510515, China: JH Wang.

Corresponding author: Correspondence to JH Wang and DF Qiao.

Authors' contributions

H Qiu: Conceptualization, Experiments, Data Collection, Statistical Analysis, Sing cell Data Analysis, Writing (Original Draft), Writing (Editing). X Yue, YB Huang and ZL Meng: Animal treatments and Behavior data analysis. JH Wang: Sing-cell Data Analysis, Funding. DF Qiao: Supervision, Funding, Writing (Editing).

Funding

Funder	Grant reference number	Author
MOST | National Natural Science Foundation of China (NSFC)	No.82271930	Dongfang Qiao
Guangdong Basic and Applied Basic Reasearch Foundation	2024A1515013050	Dongfang Qiao
Guangdong Basic and Applied Basic Reasearch Foundation	2021A1515010909	Dongfang Qiao
Guangdong Basic and Applied Basic Reasearch Foundation	2022A1515110743	Jiahong Wang

Author ORCID iDs

Hai Qiu: https://orcid.org/0009-0002-5031-7914
Yuebing Huang: https://orcid.org/0009-0001-9609-3381
Dongfang Qiao: https://orcid.org/0000-0003-2527-9039

Additional files

Supplementary file 1.

Supplementary file 2.

Supplementary file 3.

Supplementary file 4.

References

1. **UNODC TUNO** (2023) orld Drug Report 2023. www.unodc.org/unodc/en/data-and-analysis/world-drug-report-2023.html
2. **Thompson PM,** Hayashi KM, Simon SL, Geaga JA, Hong MS, Sui Y, et al.. (2004) Structural abnormalities in the brains of human subjects who use methamphetamine. *J Neurosci* **24**:6028-6036 https://doi.org/10.1523/jneurosci.0713-04.2004 | PubMed

3. **MacDuffie KE,** Brown GG, McKenna BS, Liu TT, Meloy MJ, Tawa B, et al.. (2018) Effects of HIV Infection, methamphetamine dependence and age on cortical thickness, area and volume. *Neuroimage-clin* **20**:1044-1052 https://doi.org/10.1016/j.nicl.2018.09.034 | PubMed
4. **Schwartz DL,** Mitchell AD, Lahna DL, Luber HS, Huckans MS, Mitchell SH, et al.. (2010) Global and local morphometric differences in recently abstinent methamphetamine-dependent individuals. *Neuroimage* **50**:1392-1401 https://doi.org/10.1016/j.neuroimage.2010.01.056 | PubMed
5. **Dean AC,** Groman SM, Morales AM, London ED (2013) An evaluation of the evidence that methamphetamine abuse causes cognitive decline in humans. *Neuropsychopharmacol* **38**:259-274 https://doi.org/10.1038/npp.2012.179 | PubMed
6. **Guerin AA,** Bridson T, Plapp HM, Bedi G (2023) A systematic review and meta-analysis of health, functional, and cognitive outcomes in young people who use methamphetamine. *Neurosci Biobehav R* **153** https://doi.org/10.1016/j.neubiorev.2023.105380 | PubMed
7. **Marshall JF,** Belcher AM, Feinstein EM, O'Dell SJ (2007) Methamphetamine-induced neural and cognitive changes in rodents. *Addiction* **102 Suppl 1**:61-69 https://doi.org/10.1111/j.1360-0443.2006.01780.x | PubMed
8. **Shukla M,** Vincent B (2021) Methamphetamine abuse disturbs the dopaminergic system to impair hippocampal-based learning and memory: An overview of animal and human investigations. *Neurosci Biobehav R* **131**:541-559 https://doi.org/10.1016/j.neubiorev.2021.09.016 | PubMed
9. **Jin S,** Guerrero-Juarez CF, Zhang L, Chang I, Ramos R, Kuan CH, et al.. (2021) Inference and analysis of cell-cell communication using CellChat. *Nat Commun* **12** https://doi.org/10.1038/s41467-021-21246-9 | PubMed
10. **Qiu X,** Mao Q, Tang Y, Wang L, Chawla R, Pliner HA, et al.. (2017) Reversed graph embedding resolves complex single-cell trajectories. *Nat Methods* **14**:979-982 https://doi.org/10.1038/nmeth.4402 | PubMed
11. **Van de Sande B,** Flerin C, Davie K, De Waegeneer M, Hulselmans G, Aibar S, et al.. (2020) A scalable SCENIC workflow for single-cell gene regulatory network analysis. *Nat Protoc* **15**:2247-2276 https://doi.org/10.1038/s41596-020-0336-2 | PubMed
12. **Herrmann C,** Van de Sande B, Potier D (2012) Aerts S. i-cisTarget: an integrative genomics method for the prediction of regulatory features and cis-regulatory modules. *Nucleic Acids Res* **40**:e114 https://doi.org/10.1093/nar/gks543 | PubMed
13. **Sweeney MD,** Zhao Z, Montagne A, Nelson AR, Zlokovic BV (2019) Blood-Brain Barrier: From Physiology to Disease and Back. *Physiol Rev* **99**:21-78 https://doi.org/10.1152/physrev.00050.2017 | PubMed
14. **Pang L,** Wang Y (2023) Overview of blood-brain barrier dysfunction in methamphetamine abuse. *Biomed Pharmacother* **161** https://doi.org/10.1016/j.biopha.2023.114478 | PubMed
15. **Obermeier B,** Daneman R, Ransohoff RM (2013) Development, maintenance and disruption of the blood-brain barrier. *Nat Med* **19**:1584-1596 https://doi.org/10.1038/nm.3407 | PubMed
16. **Li S,** Sheng ZH (2023) Oligodendrocyte-derived transcellular signaling regulates axonal energy metabolism. *Curr Opin Neurobiol* **80** https://doi.org/10.1016/j.conb.2023.102722 | PubMed
17. **Lezmy J,** Arancibia-Carcamo IL, Quintela-Lopez T, Sherman DL, Brophy PJ, Attwell D (2021) Astrocyte Ca(2+)-evoked ATP release regulates myelinated axon excitability and conduction speed. *Science* **374**:eabh2858 https://doi.org/10.1126/science.abh2858 | PubMed
18. **Geigenmuller JN,** Tari AR, Wisloff U, Walker TL (2024) The relationship between adult hippocampal neurogenesis and cognitive impairment in Alzheimer's disease. *Alzheimers Dement* **20**:7369-7383 https://doi.org/10.1002/alz.14179 | PubMed
19. **Gengatharan A,** Malvaut S, Marymonchyk A, Ghareghani M, Snapyan M, Fischer-Sternjak J, et al.. (2021) Adult neural stem cell activation in mice is regulated by the day/night cycle and intracellular calcium dynamics. *Cell* **184**:709-722 https://doi.org/10.1016/j.cell.2020.12.026 | PubMed

20. **Riva M,** Moriceau S, Morabito A, Dossi E, Sanchez-Bellot C, Azzam P, et al.. (2023) Aberrant survival of hippocampal Cajal-Retzius cells leads to memory deficits, gamma rhythmopathies and susceptibility to seizures in adult mice. *Nat Commun* **14** https://doi.org/10.1038/s41467-023-37249-7 | PubMed

21. **Anstotz M,** Lee SK, Maccaferri G (2022) Glutamate released by Cajal-Retzius cells impacts specific hippocampal circuits and behaviors. *Cell Rep* **39** https://doi.org/10.1016/j.celrep.2022.110822 | PubMed

22. **Rogers K** (2018) "ependymal cell". In: *Encyclopedia Britannica* Encyclopædia Britannica, Inc.

23. **Plikus MV,** Wang X, Sinha S, Forte E, Thompson SM, Herzog EL, et al.. (2021) Fibroblasts: Origins, definitions, and functions in health and disease. *Cell* **184**:3852-3872 https://doi.org/10.1016/j.cell.2021.06.024 | PubMed

24. **Yeini E,** Ofek P, Pozzi S, Albeck N, Ben-Shushan D, Tiram G, et al.. (2021) P-selectin axis plays a key role in microglia immunophenotype and glioblastoma progression. *Nat Commun* **12** https://doi.org/10.1038/s41467-021-22186-0 | PubMed

25. **Cardone J,** Le Friec G, Kemper C (2011) CD46 in innate and adaptive immunity: an update. *Clin Exp Immunol* **164**:301-311 https://doi.org/10.1111/j.1365-2249.2011.04400.x | PubMed

26. **Cope EC,** Gould E (2019) Adult Neurogenesis, Glia, and the Extracellular Matrix. *Cell Stem Cell* **24**:690-705 https://doi.org/10.1016/j.stem.2019.03.023 | PubMed

27. **Chen YJ,** Liu YL, Zhong Q, Yu YF, Su HL, Toque HA, et al.. (2012) Tetrahydropalmatine protects against methamphetamine-induced spatial learning and memory impairment in mice. *Neurosci Bull* **28**:222-232 https://doi.org/10.1007/s12264-012-1236-4 | PubMed

28. **Veschsanit N,** Yang JL, Ngampramuan S, Viwatpinyo K, Pinyomahakul J, Lwin T, et al.. (2021) Melatonin reverts methamphetamine-induced learning and memory impairments and hippocampal alterations in mice. *Life Sci* **265** https://doi.org/10.1016/j.lfs.2020.118844 | PubMed

29. **Fan XY,** Yang JY, Dong YX, Hou Y, Liu S, Wu CF (2020) Oxytocin inhibits methamphetamine-associated learning and memory alterations by regulating DNA methylation at the Synaptophysin promoter. *Addict Biol* **25**:e12697 https://doi.org/10.1111/adb.12697 | PubMed

30. **Gutierrez A,** Jablonski SA, Amos-Kroohs RM, Barnes AC, Williams MT, Vorhees CV (2017) Effects of Housing on Methamphetamine-Induced Neurotoxicity and Spatial Learning and Memory. *Acs Chem Neurosci* **8**:1479-1489 https://doi.org/10.1021/acschemneuro.6b00419 | PubMed

31. **Jayanthi S,** Daiwile AP, Cadet JL (2021) Neurotoxicity of methamphetamine: Main effects and mechanisms. *Exp Neurol* **344** https://doi.org/10.1016/j.expneurol.2021.113795 | PubMed

32. **Limanaqi F,** Busceti CL, Celli R, Biagioni F, Fornai F (2021) Autophagy as a gateway for the effects of methamphetamine: From neurotransmitter release and synaptic plasticity to psychiatric and neurodegenerative disorders. *Prog Neurobiol* **204** https://doi.org/10.1016/j.pneurobio.2021.102112 | PubMed

33. **Shrestha P,** Katila N, Lee S, Seo JH, Jeong JH, Yook S (2022) Methamphetamine induced neurotoxic diseases, molecular mechanism, and current treatment strategies. *Biomed Pharmacother* **154** https://doi.org/10.1016/j.biopha.2022.113591 | PubMed

34. **Bowyer JF,** Sarkar S, Tranter KM, Hanig JP, Miller DB, O'Callaghan JP (2016) Vascular-directed responses of microglia produced by methamphetamine exposure: indirect evidence that microglia are involved in vascular repair?. *J Neuroinflamm* **13** https://doi.org/10.1186/s12974-016-0526-6 | PubMed

35. **Ghosh M,** Pearse DD (2024) The Yin and Yang of Microglia-Derived Extracellular Vesicles in CNS Injury and Diseases. *Cells-basel* **13** https://doi.org/10.3390/cells13221834 | PubMed

36. **Chiareli RA,** Carvalho GA, Marques BL, Mota LS, Oliveira-Lima OC, Gomes RM, et al.. (2021) The Role of Astrocytes in the Neurorepair Process. *Front Cell Dev Biol* **9** https://doi.org/10.3389/fcell.2021.665795 | PubMed

37. **Lazarov O,** Hollands C (2016) Hippocampal neurogenesis: Learning to remember. *Prog Neurobiol* **138-140** https://doi.org/10.1016/j.pneurobio.2015.12.006 | PubMed

38. **Castellani G,** Croese T, Peralta RJ, Schwartz M (2023) Transforming the understanding of brain immunity. *Science* **380**:eabo7649 https://doi.org/10.1126/science.abo7649 | PubMed

39. **Uddin MS,** Lim LW (2022) Glial cells in Alzheimer's disease: From neuropathological changes to therapeutic implications. *Ageing Res Rev* **78** https://doi.org/10.1016/j.arr.2022.101622 | PubMed

40. **Lappin JM** (2025) Rare but relevant: Methamphetamine and Parkinson's disease. *Addiction* **120**:797-800 https://doi.org/10.1111/add.16695 | PubMed

41. **Shukla M,** Vincent B (2020) The multi-faceted impact of methamphetamine on Alzheimer's disease: From a triggering role to a possible therapeutic use. *Ageing Res Rev* **60** https://doi.org/10.1016/j.arr.2020.101062 | PubMed

42. **Guo D,** Huang X, Xiong T, Wang X, Zhang J, Wang Y, et al.. (2022) Molecular mechanisms of programmed cell death in methamphetamine-induced neuronal damage. *Front Pharmacol* **13** https://doi.org/10.3389/fphar.2022.980340 | PubMed

43. **Mei Y,** Yuan Z, Song B, Li D, Ma C, Hu C, et al.. (2008) Activating transcription factor 3 up-regulated by c-Jun NH(2)-terminal kinase/c-Jun contributes to apoptosis induced by potassium deprivation in cerebellar granule neurons. *Neuroscience* **151**:771-779 https://doi.org/10.1016/j.neuroscience.2007.10.057 | PubMed

44. **Falk J,** Bechara A, Fiore R, Nawabi H, Zhou H, Hoyo-Becerra C, et al.. (2005) Dual functional activity of semaphorin 3B is required for positioning the anterior commissure. *Neuron* **48**:63-75 https://doi.org/10.1016/j.neuron.2005.08.033 | PubMed

45. **Mohan V,** Wade SD, Sullivan CS, Kasten MR, Sweetman C, Stewart R, et al.. (2019) Close Homolog of L1 Regulates Dendritic Spine Density in the Mouse Cerebral Cortex Through Semaphorin 3B. *J Neurosci* **39**:6233-6250 https://doi.org/10.1523/jneurosci.2984-18.2019 | PubMed

46. **Martins LF,** Brambilla I, Motta A, de Pretis S, Bhat GP, Badaloni A, et al.. (2022) Motor neurons use push-pull signals to direct vascular remodeling critical for their connectivity. *Neuron* **110**:4090-4107 https://doi.org/10.1016/j.neuron.2022.09.021 | PubMed

47. **Herradon G,** Perez-Garcia C (2014) Targeting midkine and pleiotrophin signalling pathways in addiction and neurodegenerative disorders: recent progress and perspectives. *Brit J Pharmacol* **171**:837-848 https://doi.org/10.1111/bph.12312 | PubMed

48. **Alberini CM** (2023) IGF2 in memory, neurodevelopmental disorders, and neurodegenerative diseases. *Trends Neurosci* **46**:488-502 https://doi.org/10.1016/j.tins.2023.03.007 | PubMed

49. **Trousse F,** Jemli A, Silhol M, Garrido E, Crouzier L, Naert G, et al.. (2019) Knockdown of the CXCL12/CXCR7 chemokine pathway results in learning deficits and neural progenitor maturation impairment in mice. *Brain Behav Immun* **80**:697-710 https://doi.org/10.1016/j.bbi.2019.05.019 | PubMed

50. **Abe P,** Wust HM, Arnold SJ, van de Pavert SA, Stumm R (2018) CXCL12-mediated feedback from granule neurons regulates generation and positioning of new neurons in the dentate gyrus. *Glia* **66**:1566-1576 https://doi.org/10.1002/glia.23324 | PubMed

51. **Li M,** Hale JS, Rich JN, Ransohoff RM, Lathia JD (2012) Chemokine CXCL12 in neurodegenerative diseases: an SOS signal for stem cell-based repair. *Trends Neurosci* **35**:619-628 https://doi.org/10.1016/j.tins.2012.06.003 | PubMed

52. **Crews L,** Adame A, Patrick C, Delaney A, Pham E, Rockenstein E, et al.. (2010) Increased BMP6 levels in the brains of Alzheimer's disease patients and APP transgenic mice are accompanied by impaired neurogenesis. *J Neurosci* **30**:12252-12262 https://doi.org/10.1523/jneurosci.1305-10.2010 | PubMed

53. **Wu X,** Yao J, Wang L, Zhang D, Zhang L, Reynolds EX, et al.. (2019) Crosstalk between BMP and Notch Induces Sox2 in Cerebral Endothelial Cells. *Cells-basel* **8** https://doi.org/10.3390/cells8060549 | PubMed

54. **Li Z,** Liu G, Yang L, Sun M, Zhang Z, Xu Z, et al.. (2024) BMP7 expression in mammalian cortical radial glial cells increases the length of the neurogenic period. *Protein Cell* **15**:21-35 https://doi.org/10.1093/procel/pwad036 | PubMed

55. **Tang MM,** Lin WJ, Zhang JT, Zhao YW, Li YC (2017) Exogenous FGF2 reverses depressive-like behaviors and restores the suppressed FGF2-ERK1/2 signaling and the impaired hippocampal neurogenesis induced by neuroinflammation. *Brain Behav Immun* **66**:322-331 https://doi.org/10.1016/j.bbi.2017.05.013 | PubMed

56. **Mandyam CD,** Wee S, Crawford EF, Eisch AJ, Richardson HN, Koob GF (2008) Varied access to intravenous methamphetamine self-administration differentially alters adult hippocampal neurogenesis. *Biol Psychiat* **64**:958-965 https://doi.org/10.1016/j.biopsych.2008.04.010 | PubMed

57. **Recinto P,** Samant AR, Chavez G, Kim A, Yuan CJ, Soleiman M, et al.. (2012) Levels of neural progenitors in the hippocampus predict memory impairment and relapse to drug seeking as a function of excessive methamphetamine self-administration. *Neuropsychopharmacol* **37**:1275-1287 https://doi.org/10.1038/npp.2011.315 | PubMed

58. **Galinato MH,** Lockner JW, Fannon-Pavlich MJ, Sobieraj JC, Staples MC, Somkuwar SS, et al.. (2018) A synthetic small-molecule Isoxazole-9 protects against methamphetamine relapse. *Mol Psychiatr* **23**:629-638 https://doi.org/10.1038/mp.2017.46 | PubMed

59. **Che X,** Bai Y, Cai J, Liu Y, Li Y, Yin M, et al.. (2021) Hippocampal neurogenesis interferes with extinction and reinstatement of methamphetamine-associated reward memory in mice. *Neuropharmacology* **196** https://doi.org/10.1016/j.neuropharm.2021.108717 | PubMed

60. **Wang S,** Wang L, Bu Q, Wei Q, Jiang L, Dai Y, et al.. (2023) Methamphetamine exposure drives cell cycle exit and aberrant differentiation in rat hippocampal-derived neurospheres. *Front Pharmacol* **14** https://doi.org/10.3389/fphar.2023.1242109 | PubMed

61. **Baptista S,** Bento AR, Goncalves J, Bernardino L, Summavielle T, Lobo A, et al.. (2012) Neuropeptide Y promotes neurogenesis and protection against methamphetamine-induced toxicity in mouse dentate gyrus-derived neurosphere cultures. *Neuropharmacology* **62**:2413-2423 https://doi.org/10.1016/j.neuropharm.2012.02.015 | PubMed

62. **Bento AR,** Baptista S, Malva JO, Silva AP, Agasse F (2011) Methamphetamine exerts toxic effects on subventricular zone stem/progenitor cells and inhibits neuronal differentiation. *Rejuv Res* **14**:205-214 https://doi.org/10.1089/rej.2010.1109 | PubMed

63. **Yang Q,** Wei X, Deng B, Chang Z, Jin D, Huang Y, et al.. (2022) Cerebral small vessel disease alters neurovascular unit regulation of microcirculation integrity involved in vascular cognitive impairment. *Neurobiol Dis* **170** https://doi.org/10.1016/j.nbd.2022.105750 | PubMed

64. **McQueen A,** Warboys CM (2023) Mechanosignalling pathways that regulate endothelial barrier function. *Curr Opin Cell Biol* **84** https://doi.org/10.1016/j.ceb.2023.102213 | PubMed

65. **Li Y,** Cui Z, Liao Q, Dong H, Zhang J, Shen W, et al.. (2019) Support vector machine-based multivariate pattern classification of methamphetamine dependence using arterial spin labeling. *Addict Biol* **24**:1254-1262 https://doi.org/10.1111/adb.12705 | PubMed

66. **Lafuente JV,** Sharma A, Muresanu DF, Ozkizilcik A, Tian ZR, Patnaik R, et al.. (2018) Repeated Forced Swim Exacerbates Methamphetamine-Induced Neurotoxicity: Neuroprotective Effects of Nanowired Delivery of 5-HT3-Receptor Antagonist Ondansetron. *Mol Neurobiol* **55**:322-334 https://doi.org/10.1007/s12035-017-0744-7 | PubMed

67. **Ances BM,** Vaida F, Cherner M, Yeh MJ, Liang CL, Gardner C, et al.. (2011) HIV and chronic methamphetamine dependence affect cerebral blood flow. *J Neuroimmune Pharm* **6**:409-419 https://doi.org/10.1007/s11481-011-9270-y | PubMed

68. **Garcia FJ,** Sun N, Lee H, Godlewski B, Mathys H, Galani K, et al.. (2022) Single-cell dissection of the human brain vasculature. *Nature* **603**:893-899 https://doi.org/10.1038/s41586-022-04521-7 | PubMed

69. **Liddelow SA,** Guttenplan KA, Clarke LE, Bennett FC, Bohlen CJ, Schirmer L, et al.. (2017) Neurotoxic reactive astrocytes are induced by activated microglia. *Nature* **541**:481-487 https://doi.org/10.1038/nature21029 | PubMed

70. **Chen X,** Firulyova M, Manis M, Herz J, Smirnov I, Aladyeva E, et al.. (2023) Microglia-mediated T cell infiltration drives neurodegeneration in tauopathy. *Nature* **615**:668-677 https://doi.org/10.1038/s41586-023-05788-0 | PubMed

71. **Lee HG,** Lee JH, Flausino LE, Quintana FJ (2023) Neuroinflammation: An astrocyte perspective. *Sci Transl Med* **15**:eadi7828 https://doi.org/10.1126/scitranslmed.adi7828 | PubMed

72. **Cameron EG,** Nahmou M, Toth AB, Heo L, Tanasa B, Dalal R, et al.. (2024) A molecular switch for neuroprotective astrocyte reactivity. *Nature* **626**:574-582 https://doi.org/10.1038/s41586-023-06935-3 | PubMed

73. **Murdock MH,** Tsai LH (2023) Insights into Alzheimer's disease from single-cell genomic approaches. *Nat Neurosci* **26**:181-195 https://doi.org/10.1038/s41593-022-01222-2 | PubMed

74. **Profaci CP,** Harvey SS, Bajc K, Zhang TZ, Jeffrey DA, Zhang AZ, et al.. (2024) Microglia are not necessary for maintenance of blood-brain barrier properties in health, but PLX5622 alters brain endothelial cholesterol metabolism. *Neuron* **112**:2910-2921 https://doi.org/10.1016/j.neuron.2024.07.015 | PubMed

75. **Haney MS,** Palovics R, Munson CN, Long C, Johansson PK, Yip O, et al.. (2024) APOE4/4 is linked to damaging lipid droplets in Alzheimer's disease microglia. *Nature* **628**:154-161 https://doi.org/10.1038/s41586-024-07185-7 | PubMed

76. **Balliu B,** Durrant M, Goede O, Abell N, Li X, Liu B, et al.. (2019) Genetic regulation of gene expression and splicing during a 10-year period of human aging. *Genome Biol* **20** https://doi.org/10.1186/s13059-019-1840-y | PubMed

77. **Lananna BV,** McKee CA, King MW, Del-Aguila JL, Dimitry JM, Farias F, et al.. (2020) Chi3l1/YKL-40 is controlled by the astrocyte circadian clock and regulates neuroinflammation and Alzheimer's disease pathogenesis. *Sci Transl Med* **12** https://doi.org/10.1126/scitranslmed.aax3519 | PubMed

78. **He J,** Hsuchou H, He Y, Kastin AJ, Wang Y, Pan W (2014) Sleep restriction impairs blood-brain barrier function. *J Neurosci* **34**:14697-14706 https://doi.org/10.1523/jneurosci.2111-14.2014 | PubMed

79. **Cuddapah VA,** Zhang SL, Sehgal A (2019) Regulation of the Blood-Brain Barrier by Circadian Rhythms and Sleep. *Trends Neurosci* **42**:500-510 https://doi.org/10.1016/j.tins.2019.05.001 | PubMed

80. **Zhang SL,** Lahens NF, Yue Z, Arnold DM, Pakstis PP, Schwarz JE, et al.. (2021) A circadian clock regulates efflux by the blood-brain barrier in mice and human cells. *Nat Commun* **12** https://doi.org/10.1038/s41467-020-20795-9 | PubMed

81. **Zhang C,** Chen C, Zhao X, Lu J, Zhang M, Qiu H, et al.. (2022) New insight into methamphetamine-associated heart failure revealed by transcriptomic analyses: Circadian rhythm disorder. *Toxicol Appl Pharm* **451** https://doi.org/10.1016/j.taap.2022.116172 | PubMed

82. **Behrouzvaziri A,** Zaretskaia MV, Rusyniak DE, Zaretsky DV, Molkov YI (2018) Circadian variability of body temperature responses to methamphetamine. *Am J Physiol-reg I* **314**:R43-R48 https://doi.org/10.1152/ajpregu.00170.2017 | PubMed

83. **Rawashdeh O,** Clough SJ, Hudson RL, Dubocovich ML (2017) Learned motivation drives circadian physiology in the absence of the master circadian clock. *FASEB J* **31**:388-399 https://doi.org/10.1096/fj.201600926r | PubMed

84. **Sayson LV,** Lee HJ, Ortiz DM, Kim M, Custodio R, Lee CH, et al.. (2023) The differential vulnerabilities of Per2 knockout mice to the addictive properties of methamphetamine and cocaine. *Prog Neuro-psychoph* **126** https://doi.org/10.1016/j.pnpbp.2023.110782 | PubMed

Qiu H (2025) Hippocampal single-cell RNA Atlas of chronic methamphetamine abuse-induced cognitive decline in mice. NCBI Gene Expression Omnibus. ID GSE252939 https://www.ncbi.nlm.nih.gov/geo/query/acc.cgi?acc=GSE252939

Peer reviews

Reviewer #1 (Public review):

Summary:

The manuscript, titled Hippocampal Single-Cell RNA Atlas of Chronic Methamphetamine Abuse-Induced Cognitive Decline in Mice, focuses on single-cell RNA sequencing (scRNA-seq) analysis following chronic methamphetamine (METH) treatment in mice. The authors propose two hypotheses: (1) METH induces neuroinflammation involving T and NKT cells, and (2) METH alters neuronal stem cell differentiation.

Strengths:

The authors provide a substantial dataset with numerous replicates, offering valuable resources to the research community.

Weaknesses:

Concerns remain regarding the interpretation of the data and the appropriateness of the statistical analyses.

Although the authors provided detailed responses to the reviewer's concerns, I am still concerned that several key issues have not yet been fully addressed in the revised manuscript.

First, in Figure 5, the authors state that neural stem cells (NSCs) preferentially differentiate into astrocytes rather than neuroblasts following METH treatment. However, based on the presented trajectories, it is difficult to visually confirm differences in the relative proportions of astrocyte versus neuroblast differentiation between the control and METH-treated conditions. The current figures do not provide a quantitative or clearly interpretable comparison of lineage allocation that would support this conclusion.

Moreover, in Figures 5C and 5F, the inferred pseudotime trajectories differ both the starting cell populations and the intermediate and terminal cell identities. As a result, the trajectories are not directly comparable between the control and METH conditions. Under these circumstances, it is inappropriate to interpret gene expression changes as occurring along equivalent differentiation paths, and the current analysis does not convincingly support the stated conclusions regarding altered NSC differentiation.

If the authors intend to claim differential gene expression associated with altered differentiation trajectories, the analysis should at minimum present the expression of the same set of genes (e.g., Bsg, Ccl4, Fos, Sox11, Flt1, Hspb1, Igfbp7, and Tmsb10) plotted along a matched trajectory (for example, NSC-to-astrocyte or NSC-to-neuroblast lineages) in both control and METH-treated samples, so that readers can directly compare expression dynamics across conditions.

In addition, several statements throughout the manuscript describing changes in cell-type proportions are not supported by corresponding statistical analyses. For example, in Figure 2C (around line 430), the authors report changes in cell proportions of ~0.1% or 2-3%. Without appropriate statistical testing, it is unclear whether such marginal differences are biologically meaningful or reproducible. The authors should either provide statistical testing (e.g., sample-level proportion analysis with p-values or confidence intervals) or revise the text to describe these findings as descriptive rather than significant changes.

Finally, the reported decrease in astrocyte proportion following METH exposure (from 6.6% to 5.5%), together with the lack of reported changes in neuroblast proportions, appears

inconsistent with the trajectory-based conclusion that NSCs preferentially differentiate into astrocytes in METH-treated mice. This apparent discrepancy should be clarified or the conclusions appropriately tempered.

https://doi.org/10.7554/eLife.106940.2.sa1

Author response:

The following is the authors' response to the original reviews.

> ***Public Reviews:***
>
> ***Reviewer #1 (Public review):***
>
> *(1) Concerns persist regarding the interpretation of data and the validation of experiments. First, the presence of T cells, NKT cells, and neutrophils in both the control and METH-treated hippocampi suggests that blood contamination rather than immune cell infiltration is the cause. Since the authors claim that METH disrupts the blood-brain barrier, increasing the infiltration of these immune cells, identifying the source of these immune cells is critical.*

We sincerely appreciate the valuable suggestions you have provided. Your professional perspective impresses us. Based on your suggestion, we conducted a systematic review and in-depth analysis of the experimental process.

As you have pointed out, we believe that the T cells, NK cells and neutrophils detected in the single-cell sequencing of the mouse hippocampus may have a blood-derived origin. However, this does not mean that the presence of these cell types in the control group is abnormal, because in many literature, these cells can also be found in the hippocampus of control mice. Nevertheless, clarifying the origin and location of these cells will help to further strengthen the persuasiveness of the research hypothesis. Although there is currently no systematic discussion on the role of such cells in the field of methamphetamine neurotoxicity research, we believe that the relevant findings still have certain reference value for subsequent research in this field.

Our response is based on the following description:

(1) Insufficient perfusion during the extraction of the hippocampus may lead to a certain degree of blood contamination.

Given that the single-cell sequencing technique employed in this study can detect all the mRNA of the entire cell, in order to ensure that the cells are in the optimal physiological state and to minimize the stress response caused by the experimental operation on the cells, we perfused the anesthetized mice with cold PBS for approximately 3 min (this has been supplemented in the Materials and methods Line165-166), and completed the rapid dissection and collection of the mouse hippocampus on the ice surface within 2 min, and immediately placed it in an appropriate amount of tissue preservation solution for storage. The time of tissue perfusion might be insufficient or the perfusion volume might not be adequate, resulting in the incomplete expulsion of all the blood. Subsequently, the decomposition operations of the tissue samples were all carried out in the preservation solution or PBS buffer, which to some extent reduced the potential interference of blood components on the experimental results. Additionally, T cells, NKT cells and neutrophils in the capillary perivascular spaces of the hippocampal tissue might still remain and be successfully captured, and were reflected in the final sequencing data.

(2) The presence of T cells, NKT cells, and neutrophils in the brain tissue of normal mice has been supported by existing literature. Moreover, several studies have specifically described

the localization of these immune cell types within the brain parenchyma.

Contemporary studies have completely changed the view of brain immunity from envisioning the brain as isolated and inaccessible to peripheral immune cells to an organ in close physical and functional communication with the immune system for its maintenance, function, and repair. Circulating immune cells reside in special niches in the brain's borders, the choroid plexus, meninges, and perivascular spaces, from which they patrol and sense the brain in a remote manner [1].

A large-scale mouse brain cell atlas study also reported that approximately 8% of non-neuronal cells are immune cells, including microglia, boundary-associated macrophages, lymphocytes, dendritic cells, and monocytes [2].

Hang Yao et al. demonstrated through flow cytometry that neutrophils were present in the hippocampal tissues of both healthy control mice and depressed mice (Fig.2 H) [3]. Wei Su et al. identified through single-cell sequencing that dendritic cells, neutrophils, macrophages, T cells, and NKT cells were present in the brain tissues of non-transgenic (Non-Tg) control mice (Fig.1a-b), and the localization of these cells was explicitly characterized as brain parenchyma in the study [4]. Tomomi M Yoshida et al. discovered through immunohistochemistry (IHC) and single-cell sequencing techniques that there were a certain number of CD3+ and CD4+ T cells in the hippocampus and other regions of the brain, and they observed that these cells were located outside the blood vessels. (Fig.1a-c, g) [5].

(3) Both the analysis of immune cells within blood vessels and those in the brain parenchyma contribute to elucidating the immune effects in the hippocampal microenvironment under chronic METH exposure, as well as their interactions with other cell types. At present, the understanding of the neurotoxicity of methylphenidate and the immune system is still limited to the central resident immune cells, such as microglia, astrocytes and oligodendrocytes [6]. Adaptive immune cells and myeloid cells recruited from the circulation have also been implicated in brain development, function, and aging. Their depletion during developmental stages can disrupt critical neural processes, including glial cell maturation, neuronal activity, and myelinogenesis. However, the precise developmental stage at which lymphocyte infiltration into the central nervous system occurs remains to be elucidated [7].

Our data results indicate that during chronic METH abuse, T cells are more active and participate in the regulation of cytokines through complement signaling. At the same time, the frequency of cell communication between endothelial cells and epithelial cells is increased. Moreover, microglia upregulated the processes of cell chemotaxis and migration, as well as the communication with immune cells such as T cells, and to some extent, this also suggests an enhanced infiltration of T cells. However, we also recognize that the current conclusions regarding immune cell infiltration based on sequencing data and literature reports lack the support of experimental data. Currently, we are conducting morphological analysis using the same batch of brain tissue samples to further validate the relevant findings.

Immune fluorescence staining and flow cytometry can be utilized to further determine the locations of these immune cells in the hippocampus. The classical pathways through which peripheral immune cells enter the brain mainly include the BBB and the choroid plexus. In June 2025, Kim N. Green et al. published a study in Neuron, further revealing that during the developmental stage and in cases of inflammatory diseases, immune cells can also infiltrate the brain parenchyma through a newly identified channel - the medial ventricle, thereby further confirming that these cells have the ability to migrate to the central nervous system under specific physiological or pathological conditions [8].

(1) Castellani G, Croese T, Peralta Ramos JM, Schwartz M. Transforming the understanding of brain immunity. Science. 2023 Apr 7;380(6640):eabo7649. doi: 10.1126/science.abo7649.

(2) Zhang M, Pan X, Jung W, Halpern AR, Eichhorn SW, Lei Z, Cohen L, Smith KA, Tasic B, Yao Z, Zeng H, Zhuang X. Molecularly defined and spatially resolved cell atlas of the whole mouse brain. Nature. 2023 Dec;624(7991):343-354. doi: 10.1038/s41586-023-06808-9.

(3) Yao H, Jiang SY, Jiao YY, Zhou ZY, Zhu Z, Wang C, Zhang KZ, Ma TF, Hu G, Du RH, Lu M. Astrocyte-derived CCL5-mediated CCR5+ neutrophil infiltration drives depression pathogenesis. Sci Adv. 2025 May 23;11(21):eadt6632. doi: 10.1126/sciadv.adt6632.

(4) Su W, Saravia J, Risch I, Rankin S, Guy C, Chapman NM, Shi H, Sun Y, Kc A, Li W, Huang H, Lim SA, Hu H, Wang Y, Liu D, Jiao Y, Chen PC, Soliman H, Yan KK, Zhang J, Vogel P, Liu X, Serrano GE, Beach TG, Yu J, Peng J, Chi H. CXCR6 orchestrates brain CD8+ T cell residency and limits mouse Alzheimer's disease pathology. Nat Immunol. 2023 Oct;24(10):1735-1747. doi: 10.1038/s41590-023-01604-z.

(5) Yoshida TM, Nguyen M, Zhang L, Lu BY, Zhu B, Murray KN, Mineur YS, Zhang C, Xu D, Lin E, Luchsinger J, Bhatta S, Waizman DA, Coden ME, Ma Y, Israni-Winger K, Russo A, Wang H, Song W, Al Souz J, Zhao H, Craft JE, Picciotto MR, Grutzendler J, Distasio M, Palm NW, Hafler DA, Wang A. The subfornical organ is a nucleus for gut-derived T cells that regulate behaviour. Nature. 2025 Jul;643(8071):499-508. doi: 10.1038/s41586-025-09050-7.

(6) Shi S, Sun Y, Zan G, Zhao M. The interaction between central and peripheral immune systems in methamphetamine use disorder: current status and future directions. J Neuroinflammation. 2025 Feb 15;22(1):40. doi: 10.1186/s12974-025-03372-z.

(7) Castellani G, Croese T, Peralta Ramos JM, Schwartz M. Transforming the understanding of brain immunity. Science. 2023 Apr 7;380(6640):eabo7649. doi: 10.1126/science.abo7649.

(8) Hohsfield LA, Kim SJ, Barahona RA, Henningfield CM, Mansour K, Vallejo KD, Tsourmas KI, Kwang NE, Ghorbanian Y, Angulo JAA, Gao P, Pachow C, Inlay MA, Walsh CM, Xu X, Lane TE, Green KN. Identification of the velum interpositum as a meningeal-CNS route for myeloid cell trafficking into the brain. Neuron. 2025 May 28:S0896-6273(25)00351-4. doi: 10.1016/j.neuron.2025.05.004.

> *(2) Secondly, the pseudotime analysis, which suggests altered neural stem cell (NSC) differentiation, is not conclusively supported by the current data and requires further validation.*

We sincerely appreciate your valuable feedback, which we find highly relevant and constructive. It is important to acknowledge that the sequencing data presented in our study currently lacks experimental validation. Nevertheless, considering that existing research on the effects of METH on neural stem cell differentiation predominantly emphasizes observational phenomena and remains limited in terms of *in vivo* experimental evidence and mechanistic investigations, we aim to contribute our analytical findings as a reference for further scholarly exploration in this field.

Our study utilized pseudotime analysis (powered by Monocle2) to reconstruct an "imaginary timeline" (pseudo-time) based on intercellular gene expression similarities, thereby modeling the dynamic state transitions of cells during continuous biological processes. Drawing upon single-cell RNA sequencing data captured as "snapshots" from hippocampal astrocytes, neural stem cells, and neuroblasts in mice four weeks after METH exposure, we applied computational algorithms to integrate the originally discrete cellular states into a continuous pseudo-time trajectory. This approach was employed to elucidate the differentiation stages of these cell populations, identify potential branching points in their developmental pathways, and uncover the key regulatory genes driving the differentiation process. Pseudotime analysis, as a computational approach grounded in mathematical modeling, yields inferences that are contingent upon the underlying assumptions of the algorithms employed.

Consequently, experimental validation through methodologies such as time-series sampling and lineage tracing is essential to substantiate the derived biological interpretations. In light of the insufficiency of such empirical verification to date, our conclusions concerning alterations in the dynamic behavior of neural stem cell differentiation remain preliminary and require further experimental support.

In Figures 5C and 5F, we present the expression profiles of the four genes exhibiting the most statistically significant differences across the differentiation trajectory. In Figures 5B and 5E, we conducted GO and KEGG functional enrichment analyses on the genes that showed significant differential expression at different differentiation stages. While no studies within the current METH research domain have reported on the potential effects of these genes on neural stem cell differentiation, emerging evidence from related fields provides preliminary insights into their functional roles. For instance, the *Flt1* gene (also known as *VEGFR1*), referred to as the vascular endothelial growth factor receptor, has been demonstrated to play a critical role in the conversion of Müller glial cells into neurons within the zebrafish retina [1], serves as a critical regulator in promoting definitive neural stem cell survival [2]. Furthermore, it substantiates the intricate interconnection between neurons, neural stem cells, and vascular cells, as identified in our cell communication analysis. *Hsp1b* gene plays a significant role in ferroptosis and autophagy processes of nerve cells[3, 4], and may be closely related to the self-renewal ability of neural stem cell, while METH may impair neural stem cell function by disrupting autophagy, leading to reduced self-renewal capacity and altered differentiation potential [5]. In METH group, *Sox11* has been shown to play a critical role in early differentiation and neuronal growth, both during perinatal development and in adult neurogenesis [6] *Fos* gene plays a critical regulatory role in the differentiation of neural stem cells into neurons and in modulating neuronal functional activities [7]; Alterations in *Ccl5* expression levels may indicate astrocyte-mediated inflammatory responses, which could represent one of the underlying mechanisms through which METH promotes the differentiation of neural stem cells into astrocytes.

Thank you very much for your thoughtful questions and valuable suggestions. These suggestions have helped us gain a deeper understanding of the areas where we can improve, and have guided us toward more meaningful directions for future research.

(1) Mitra S, Devi S, Lee MS, Jui J, Sahu A, Goldman D. Vegf signaling between Müller glia and vascular endothelial cells is regulated by immune cells and stimulates retina regeneration. Proc Natl Acad Sci U S A. 2022 Dec 13;119(50):e2211690119. doi: 10.1073/pnas.2211690119.

(2) Wada T, Haigh JJ, Ema M, Hitoshi S, Chaddah R, Rossant J, Nagy A, van der Kooy D. Vascular endothelial growth factor directly inhibits primitive neural stem cell survival but promotes definitive neural stem cell survival. J Neurosci. 2006 Jun 21;26(25):6803-12. doi: 10.1523/JNEUROSCI.0526-06.2006.

(3) Meng J, Fang J, Bao Y, Chen H, Hu X, Wang Z, Li M, Cheng Q, Dong Y, Yang X, Zou Y, Zhao D, Tang J, Zhang W, Chen C. The biphasic role of Hspb1 on ferroptotic cell death in Parkinson's disease. Theranostics. 2024 Aug 1;14(12):4643-4666. doi: 10.7150/thno.98457.

(4) Sisto A, van Wermeskerken T, Pancher M, Gatto P, Asselbergh B, Assunção Carreira ÁS, De Winter V, Adami V, Provenzani A, Timmerman V. Autophagy induction by piplartine ameliorates axonal degeneration caused by mutant HSPB1 and HSPB8 in Charcot-Marie-Tooth type 2 neuropathies. Autophagy. 2025 May;21(5):1116-1143. doi: 10.1080/15548627.2024.2439649.

(5) Gu C, Wang Z, Luo W, Ling H, Cui X, Deng T, Li K, Huang W, Xie Q, Tao B, Qi X, Peng X, Ding J, Qiu P. Impaired olfactory bulb neurogenesis mediated by Notch1 contributes to olfactory dysfunction in mice chronically exposed to methamphetamine. Cell Biol Toxicol. 2025 Feb 20;41(1):46. doi: 10.1007/s10565-025-10004-y.

(6) Rasetto NB, Giacomini D, Berardino AA, Waichman TV, Beckel MS, Di Bella DJ, Brown J, Davies-Sala MG, Gerhardinger C, Lie DC, Arlotta P, Chernomoretz A, Schinder AF. Transcriptional dynamics orchestrating the development and integration of neurons born in the adult hippocampus. Sci Adv. 2024 Jul 19;10(29):eadp6039. doi: 10.1126/sciadv.adp6039.

(7) Pagin M, Pernebrink M, Pitasi M, Malighetti F, Ngan CY, Ottolenghi S, Pavesi G, Cantù C, Nicolis SK. FOS Rescues Neuronal Differentiation of Sox2-Deleted Neural Stem Cells by Genome-Wide Regulation of Common SOX2 and AP1(FOS-JUN) Target Genes. Cells. 2021 Jul 12;10(7):1757. doi: 10.3390/cells10071757.

> ***Reviewer #2 (Public review):***
>
> *(1) Despite this potential novelty, the study has numerous weaknesses. Notably, single-cell RNA sequencing was unable to capture an adequate number of neuronal populations. Neurons accounted for only approximately 0.6% of the total nuclei, representing a significant underrepresentation compared to their actual physiological proportion. Given that the behavioral effects of METH are likely mediated by neuronal dysfunction, readers would reasonably expect to see transcriptional changes in neurons. The authors should explain why they were unable to capture a sufficient number of neurons and justify how this incomplete dataset can still provide meaningful scientific insights for researchers studying METH-induced hippocampal damage and behavioral alterations.*

Thank you sincerely for bringing this important issue to our attention.

Firstly, this represents an unavoidable technical bottleneck. The single-cell sequencing (scRNA-seq) we perform involves the detection of mRNA at the whole-cell level, a process that necessitates cells with high structural integrity, robust viability, and minimal exposure to external stimuli. During the preparation of single-cell suspensions, mature neurons due to their highly differentiated state, morphological rigidity, and excessively long axons often fail to maintain structural integrity. These cells typically undergo death during the dissociation process, lose viability, and are subsequently excluded prior to sequencing. To retain a substantial amount of neuron-related data, an alternative technique single-cell nuclear sequencing (snRNA-seq) should be employed. This method does not necessitate cell viability and focuses exclusively on the nuclei of individual cells, thereby capturing mRNA information solely from the nuclear compartment. Consequently, mRNA data originating from the cytoplasm and organelles will not be represented.

Secondly, numerous studies have shown that the neurological damage caused by chronic exposure to methamphetamine exhibits a high degree of similarity in clinical manifestations and pathogenesis to neurodegenerative diseases (such as Alzheimer's disease, Parkinson's disease, etc.) [1-4].

We fully acknowledge the central role of neurons in cognitive functions and the pathogenesis of cognitive disorders. However, despite decades of neuron-centric research that has yielded significant advancements, major challenges remain in elucidating disease origins, identifying early pathological events, and developing effective therapeutic strategies. For example, current models fail to adequately explain early disease events. Many pathological hallmarks of cognitive disorders such as amyloid plaques, neurofibrillary tangles, and α-synuclein aggregation emerge in the extracellular space long before overt neuronal loss or dysfunction occurs, and are increasingly recognized to be initiated or modulated by non-neuronal cells, including astrocytes and microglia [5]. Furthermore, the critical contribution of the neural microenvironment is often overlooked. Neuronal function and survival are highly dependent on this microenvironment, which is predominantly established and maintained by non-neuronal cell types such as astrocytes, oligodendrocytes, microglia, vascular endothelial cells,

pericytes, and interstitial cells and matrix [6-10]. Additionally, systemic factors such as metabolic dysregulation, peripheral inflammation, and vascular pathology are closely associated with cognitive disorders. These factors often initially impact non-neuronal cells, particularly those forming the blood-brain barrier (e.g., endothelial cells) or mediating immune responses (e.g., microglia), before exerting downstream effects on neurons [11,12]. Finally, current therapeutic approaches for neuron face significant limitations, highlighting an urgent need for novel intervention strategies.

During the development of neurodegenerative chronic diseases, although the structural or functional abnormalities of neurons are the direct factors leading to clinical symptoms (such as cognitive decline), this process is often regulated by various auxiliary cell types such as glial cells, immune cells, and stromal cells, and constitutes a complex pathological mechanism network. It is worth noting that the chronic and persistent progression of the disease usually results from the failure of these auxiliary cells to effectively provide support and nutrition to neurons, and even in some pathological states, they transform into effector cells that promote neuronal damage [13,14]. In recent years, a growing number of evidence has demonstrated that glial cells, immune cells, and stromal cells exert critical regulatory functions in the pathogenesis of neurodegenerative diseases. These cell types not only contribute to the maintenance of neural microenvironmental homeostasis during the early stages of disease progression but also display substantial functional heterogeneity in modulating inflammatory responses, synaptic plasticity, the repair of neuronal injury, linking genetic risks with environmental factors and the pathogenic mechanism of pathological protein propagation [15-19]. These research results indicate that they have the potential to become key therapeutic targets in clinical interventions: 1. compared to neurons themselves, they are more susceptible to being targeted by drugs or biological agents (such as antibodies), and have higher accessibility; 2. Non-neuronal cells (especially glial cells) exhibit high plasticity and reactivity during the course of diseases, providing an opportunity window for intervening in their functional states (such as inhibiting harmful activation and promoting protective functions); 3. they can serve as early intervention targets before irreversible damage occurs to neurons, helping to prevent or delay the progression of the disease;4. intervention methods targeting these targets are diverse, including immunomodulation, anti-inflammatory, vascular protection, and metabolic regulation strategies, which are usually more feasible in practical applications than directly protecting the fragile neurons.

Early pharmacological studies have extensively characterized the neurotoxic effects of METH, including the induction of autophagy, apoptosis, oxidative stress, endoplasmic reticulum stress, and dopaminergic neurotoxicity [20]. However, therapeutic options and pharmacological interventions for METH abuse remain limited [21]. In recent years, increasing attention has been directed toward the impact of METH on non-neuronal cells. Research into mechanisms such as neuroinflammatory responses, blood-brain barrier disruption, and immune modulation is progressively contributing to a more comprehensive understanding of METH-induced neural injury [22-24]. Moreover, METH is a substance that induces widespread damage across multiple organ systems and diverse cell types throughout the body. Beyond its effects on neurons, various cell types exhibit distinct responses to METH exposure, which differ significantly depending on the duration of exposure. Our research dataset encompasses high-quality whole-cell mRNA sequencing data from multiple cell types within the hippocampus of mice subjected to chronic METH exposure, offering substantial data support and a robust foundation for in-depth investigation into the pathological mechanisms underlying METH-induced neurodamage.

Thirdly, the selection of scRNA-seq was guided by our experimental objectives and prior research experience. Our earlier investigations have primarily centered on astrocytes, endothelial cells, and microglia. This single-cell sequencing study is intended to enhance our understanding of these neural support cells, comprehensively explore their underlying mechanisms and cellular interactions, and ultimately provide a solid foundation and

reference for future research. However, our experience and infrastructure in the field of neuronal research remain relatively limited. To ensure the generation of high-quality data and to systematically advance the experimental objectives, we have prioritized the analysis of the neural microenvironment as the central focus of this study.

Fourthly, the hippocampal region is a brain area with highly specialized and collaborative characteristics, which can be further divided into the ventral hippocampus, the dorsal hippocampus, and multiple subregions such as DG, CA1, CA2, and CA3. The neurons in these subregions exhibit strong heterogeneity, and the experimental methods we currently adopt are still unable to precisely distinguish the neurons in these different regions, which may to some extent affect the accuracy of data interpretation. To address the impact of neuronal heterogeneity, we believe that single-cell spatial transcriptomics technology can be adopted for in-depth research. However, due to the high cost of this technology, it is currently difficult to apply it in our research group.

(1) Lappin JM. Rare but relevant: Methamphetamine and Parkinson's disease. Addiction. 2025 Apr;120(4):797-800. doi: 10.1111/add.16695. Epub 2024 Oct 22. PMID: 39434702.

(2) Lappin JM, Darke S. Methamphetamine and heightened risk for early-onset stroke and Parkinson's disease: A review. Exp Neurol. 2021 Sep;343:113793. doi: 10.1016/j.expneurol.2021.113793. Epub 2021 Jun 21. PMID: 34166684.

(3) Shukla M, Vincent B. The multi-faceted impact of methamphetamine on Alzheimer's disease: From a triggering role to a possible therapeutic use. Ageing Res Rev. 2020 Jul;60:101062. doi: 10.1016/j.arr.2020.101062.

(4) Shrestha P, Katila N, Lee S, Seo JH, Jeong JH, Yook S. Methamphetamine induced neurotoxic diseases, molecular mechanism, and current treatment strategies. Biomed Pharmacother. 2022 Oct;154:113591. doi: 10.1016/j.biopha.2022.113591.

(5) Gabitto MI, et al.. Integrated multimodal cell atlas of Alzheimer's disease. Nat Neurosci. 2024 Dec;27(12):2366-2383. doi: 10.1038/s41593-024-01774-5.

(6) Stogsdill JA, Harwell CC, Goldman SA. Astrocytes as master modulators of neural networks: Synaptic functions and disease-associated dysfunction of astrocytes. Ann N Y Acad Sci. 2023 Jul;1525(1):41-60. doi: 10.1111/nyas.15004.

(7) Terreros-Roncal J, et al.. Impact of neurodegenerative diseases on human adult hippocampal neurogenesis. Science. 2021 Nov 26;374(6571):1106-1113. doi: 10.1126/science.abl5163.

(8) Zhu K, Fu Y, Zhao Y, Niu B, Lu H. Perineuronal nets: Role in normal brain physiology and aging, and pathology of various diseases. Ageing Res Rev. 2025 Jun;108:102756. doi: 10.1016/j.arr.2025.102756.

(9) Depp C, Doman JL, Hingerl M, Xia J, Stevens B. Microglia transcriptional states and their functional significance: Context drives diversity. Immunity. 2025 May 13;58(5):1052-1067. doi: 10.1016/j.immuni.2025.04.009.

(10) Sweeney MD, Zhao Z, Montagne A, Nelson AR, Zlokovic BV. Blood-Brain Barrier: From Physiology to Disease and Back. Physiol Rev. 2019 Jan 1;99(1):21-78. doi: 10.1152/physrev.00050.2017.

(11) Nation DA, et al.. Blood-brain barrier breakdown is an early biomarker of human cognitive dysfunction. Nat Med. 2019 Feb;25(2):270-276. doi: 10.1038/s41591-018-0297-y.

(12) Montagne A, Zhao Z, Zlokovic BV. Alzheimer's disease: A matter of blood-brain barrier dysfunction? J Exp Med. 2017 Nov 6;214(11):3151-3169. doi: 10.1084/jem.20171406. Epub 2017

Oct 23.

(13) Huang Q, Wang Y, Chen S, Liang F. Glycometabolic Reprogramming of Microglia in Neurodegenerative Diseases: Insights from Neuroinflammation. Aging Dis. 2024 May 7;15(3):1155-1175. doi: 10.14336/AD.2023.0807.

(14) Shi FD, Yong VW. Neuroinflammation across neurological diseases. Science. 2025 Jun 19;388(6753):eadx0043. doi: 10.1126/science.adx0043.

(15) Xu X, Mei B, Yang Y, Li J, Weng J, Yang Y, Zhu Q, Zhang H, Liu X. Astrocytes Lingering at a Crossroads: Neuroprotection and Neurodegeneration in Neurocognitive Dysfunction. Int J Biol Sci. 2025 Apr 28;21(7):3122-3143. doi: 10.7150/ijbs.109315.

(16) Bedolla A, et al.. Adult microglial TGFβ1 is required for microglia homeostasis via an autocrine mechanism to maintain cognitive function in mice. Nat Commun. 2024 Jun 21;15(1):5306. doi: 10.1038/s41467-024-49596-0.

(17) Castellani G, Croese T, Peralta Ramos JM, Schwartz M. Transforming the understanding of brain immunity. Science. 2023 Apr 7;380(6640):eabo7649. doi: 10.1126/science.abo7649.

(18) Chen YH, Jin SY, Yang JM, Gao TM. The Memory Orchestra: Contribution of Astrocytes. Neurosci Bull. 2023 Mar;39(3):409-424. doi: 10.1007/s12264-023-01024-x.

(19) Deng Q, Wu C, Parker E, Liu TC, Duan R, Yang L. Microglia and Astrocytes in Alzheimer's Disease: Significance and Summary of Recent Advances. Aging Dis. 2024 Aug 1;15(4):1537-1564. doi: 10.14336/AD.2023.0907.

(20) Jayanthi S, Daiwile AP, Cadet JL. Neurotoxicity of methamphetamine: Main effects and mechanisms. Exp Neurol. 2021 Oct;344:113795. doi: 10.1016/j.expneurol.2021.113795.

(21) Paulus MP, Stewart JL. Neurobiology, Clinical Presentation, and Treatment of Methamphetamine Use Disorder: A Review. JAMA Psychiatry. 2020 Sep 1;77(9):959-966. doi: 10.1001/jamapsychiatry.2020.0246.

(22) Shi S, Sun Y, Zan G, Zhao M. The interaction between central and peripheral immune systems in methamphetamine use disorder: current status and future directions. J Neuroinflammation. 2025 Feb 15;22(1):40. doi: 10.1186/s12974-025-03372-z.

(23) Pang L, Wang Y. Overview of blood-brain barrier dysfunction in methamphetamine abuse. Biomed Pharmacother. 2023 May;161:114478. doi: 10.1016/j.biopha.2023.114478.

(24) Shaerzadeh F, Streit WJ, Heysieattalab S, Khoshbouei H. Methamphetamine neurotoxicity, microglia, and neuroinflammation. J Neuroinflammation. 2018 Dec 12;15(1):341. doi: 10.1186/s12974-018-1385-0.

> *(2) Another significant weakness of this study is the lack of a cohesive hypothesis or overarching conclusion regarding how METH impacts neural populations. The authors provide a largely descriptive account of transcriptional alterations across various cell types, but the manuscript lacks clear, biologically meaningful conclusions. This descriptive approach makes it difficult for readers to identify the key findings or take-home messages. To improve clarity and impact, the authors should focus on developing and presenting a few plausible hypotheses or mechanistic scenarios regarding METH-induced neurotoxicity, grounded in their scRNA-seq data. Including schematic figures to illustrate these hypotheses would also help readers better understand and interpret the study.*

We sincerely appreciate your valuable comments on our article. As you pointed out, the current research lacks experimental verification to further support our conclusions. To

enhance the clarity and readability of the mechanism explanation, we have added several hypothetical diagrams (such as Figures.7, 8, and 9) in the discussion section to present the biological mechanisms reflected by the data more intuitively. Additionally, relevant verification work is underway, such as marking specific cell types with marker proteins. Author response image 1 shows some of our preliminary experimental results that have not been published yet, and their trends are consistent with the conclusions of this article. However, since the complete verification still requires a certain period of time, to ensure the rigor of the data, these results have not been included in the current manuscript for the time being. Finally, we would like to thank you again for your constructive suggestions.

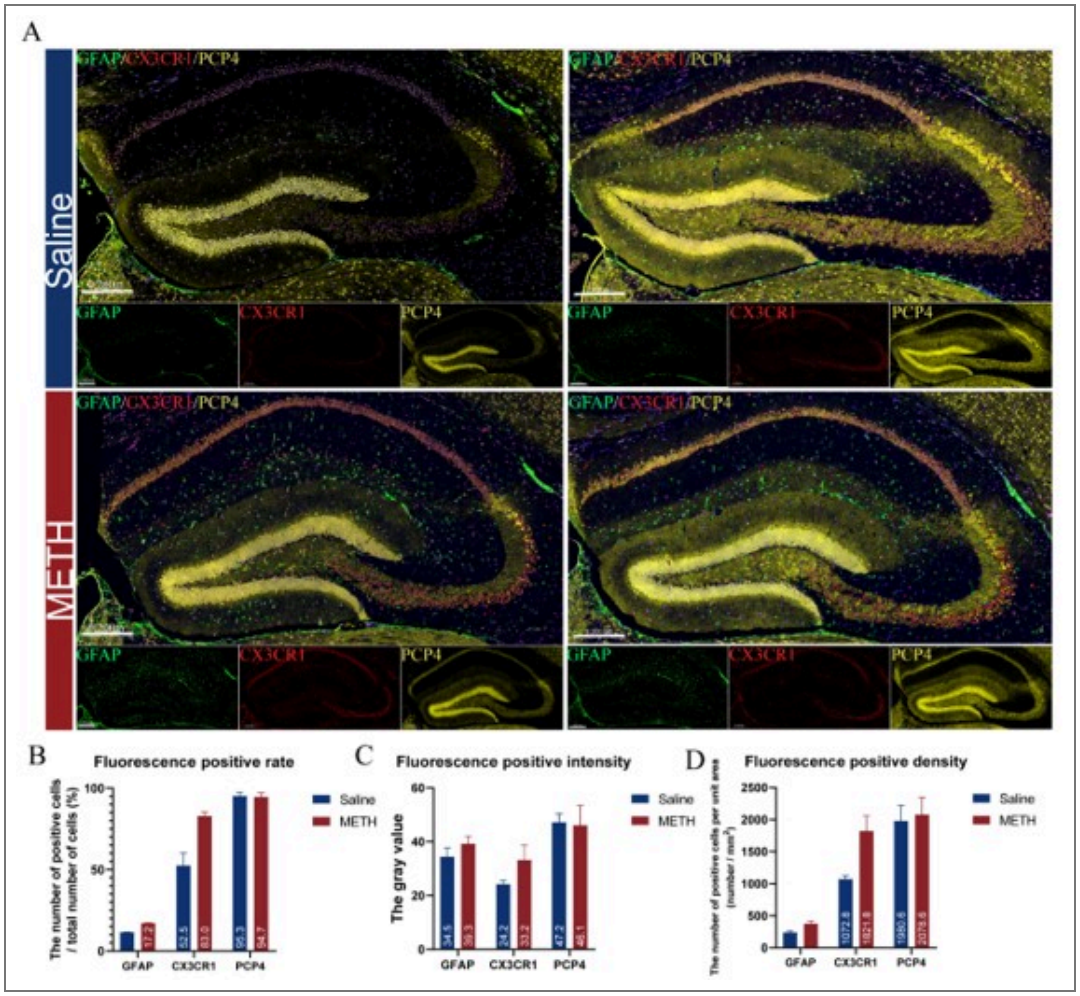

Author response image 1.

> *(3) The final major weakness of this study is its poor readability. It appears that the authors did not adequately proofread the manuscript, as there are numerous typographical errors (e.g., line 333: trisulting; line 756: essencial), unsupported scientific claims lacking citations (e.g., lines 485, 503, 749-753), and grammatically incorrect sentences (e.g., lines 470-472, 540-543, 749-753). In addition, many paragraphs are unorganized and overly descriptive, which further hinders clarity. Some figures are also problematic - too small in size and overcrowded with text in fonts that are difficult to read. It is recommended that the authors carry out quality control. There are too many typographical and grammatical errors to list individually; the authors should carefully review and revise the entire manuscript to address all of these issues.*

We truly appreciate your thoughtful feedback and sincerely apologize for any inconvenience experienced by you and other readers.

The text of this research manuscript was manually entered, which unfortunately resulted in some spelling and grammatical errors. In response, we have carefully revised the entire manuscript using word processing tools in the second version. Meanwhile, we have restructured and organized some lengthy paragraphs to enhance the clarity and readability of the content.

Regarding the issue you raised about certain viewpoints lacking citation support, we have added the necessary references to those sections and reviewed the entire text to ensure all scientific claims are properly supported.

As for the image clarity, we made sure the submitted images met the 600dpi resolution requirement. However, we acknowledge that there were clarity issues in the final published version. We have since re-adjusted and re-uploaded the images to improve their quality.

We are committed to continuously improving the manuscript and enhancing the overall quality of our academic presentation. Thank you sincerely for your kind attention to our work, your careful review, and the valuable suggestions you provided.

> ***Reviewer #3 (Public review):***
>
> *(1) While the bioinformatics analyses are extensive, the study is primarily descriptive at the molecular level. The absence of experimental validation, such as targeted mRNA/protein quantification and gene knockdown/overexpression to confirm the causal relationship between these identified genes and METH-induced cognitive deficits, is a notable limitation.*

We sincerely appreciate your valuable comments and suggestions. Indeed, there are still certain limitations in our manuscript in some aspects. It may not be able to systematically answer specific questions, and it is also difficult to fully clarify the functional roles of certain genes or specific cell types through experimental evidence.

Although our manuscript still has certain limitations, we believe that the publication of this research is expected to provide new perspectives and theoretical support for the in-depth exploration of METH toxicity damage-related fields, thereby promoting the progress of research in this direction：

(1) At present, the single-cell sequencing datasets on chronic damage caused by METH are still relatively limited, especially in terms of studies at the whole-cell level. Our dataset is expected to fill the research gap in this field to some extent, providing reference and support for subsequent related research.

(2) During the sampling process of the sequencing experiment, we ensured high cell viability and sequencing quality. The experiment exhibited good reproducibility (each group consisted of 10 mice, and 2 mice from each group were selected to mix their hippocampal tissues into one sample), and the obtained data had high credibility.

(3) The effects of METH have a wide distribution pattern across various organs and tissues. Through single-cell sequencing data, the common and differential expression patterns of related genes under different conditions can be systematically analyzed, which is helpful for future targeted knockout studies of these genes and provides a predictive basis for the evaluation of intervention measures, thereby enabling precise regulation of gene functions.

(4) This is conducive to the orderly implementation of our subsequent research plans. Our subsequent research plan can be further developed based on a specific aspect of this study.

We are indeed planning to do exactly that. During our earlier research on astrocytes, we discovered that astrocytes have two phenotypes (protective and inflammatory) in neuroinflammation. Given that astrocytes in the hippocampus show great variability depending on their location, the cells they come into contact with, and the stimuli they receive, we aim to investigate the changes in the function of astrocyte subpopulations in chronic METH-induced cognitive impairment. We focused on the role of the cAMP signaling pathway in the transformation of astrocyte phenotypes and attempted to link changes in astrocyte energy metabolism to their inflammatory phenotype. In addition, we found that endothelial cells can be easily distinguished into many subpopulations, which are related to their specific functions in immune responses, material transport, vascular growth regulation, energy metabolism, and other processes. We believe that single-cell technology can help us find the key mechanisms and intervention targets of chronic METH abuse-induced damage with greater precision.

> *(2) While the discussion extensively covers the functional implications of specific molecular pathways and cell types, it would greatly benefit from a comparison of these findings with existing RNA sequencing data from other METH models in hippocampal tissue.*

We are very grateful for your professional suggestions, which have been of great help in improving the quality of our manuscript. We agree that comparing our findings with existing RNA sequencing data from other METH models in hippocampal tissue would strengthen the discussion. In response to your suggestion, we have actively reviewed relevant literature and databases, and attempted to request the database administrators and original authors for the download and use of the relevant data. However, as data integration still requires some time, we may not be able to conduct a detailed analysis of the data in this revised version. We can only discuss the conclusions of some authors.

Palsamy Periyasamy et al. published a scRNA sequencing (live-cell) study on chronic METH exposure almost at the same time as us. They also adopted a similar gradual incremental 4-week METH exposure model and conducted sequencing analysis on glial cells in the cerebral cortex of mice [1]. The changes they observed in the circadian rhythm, adherens junctions, Rap1 signaling pathway, and cAMP signaling pathway (Disscusion, Lines 892-897) in the cortical astrocytes were also similar in the astrocytes of the hippocampal region that we studied. Similarly, in oligodendrocytes, we observed an upregulation trend of key genes regulating the circadian rhythm, such as Per2, Per3, and Nr1d1 (Disscusion, Lines 916-939). This result is consistent with their research findings. Non etheless, we believe that the changes in oligodendrocytes in terms of metabolic regulation and axonal function homeostasis are more significant.

Pingming Qiu et al. further confirmed the correlation between the NF-κB signaling pathway in hippocampal astrocytes under METH action and neuroinflammation, neuroinjury, and learning and memory impairments in mice by integrating the GEO dataset [2]. This conclusion is also consistent with the sequencing results and analysis conclusions we obtained (Results, Lines 473-476).

In terms of the neuro-immune system disorder caused by chronic METH exposure, our research findings are consistent with those of Biao Wang et al [3]. We both observed that METH exposure may involve the participation of related immune cells (such as T cells, monocytes) and may be related to the regulation of the innate immune response and the homeostasis of myeloid cells, etc. Through the identification and analysis of cell subtypes, we further revealed that these signals may be closely related to the interaction between microglia and other immune cells mediated by MHC molecules (Disscusion, Lines 870-894).

Currently, the research results related to METH are still scattered and lack systematicness. There are differences among the research models, and there are relatively few studies on

chronic exposure and *in vivo* experiments. Sequencing data sets with strong correlations are also scarce. We hope that this dataset can comprehensively and elaborately depict the molecular map of the hippocampus of mice after chronic METH exposure (although due to technical limitations, mature neurons die during dissociation, thus making it impossible to obtain the relevant data). In addition, we also hope to integrate the single-cell sequencing data and spatial transcriptome data of the hippocampus of mice after chronic METH exposure, providing a reliable data foundation and theoretical support for subsequent research in this field.

Finally, we would like to express our sincere gratitude for your valuable suggestions and support. Although we still need some time to further refine the manuscript based on your opinions, we sincerely hope that more readers will provide us with constructive feedback to promote the continuous improvement and deepening of this research.

(1) Oladapo A, Deshetty UM, Callen S, Buch S, Periyasamy P. Single-Cell RNA-Seq Uncovers Robust Glial Cell Transcriptional Changes in Methamphetamine-Administered Mice. Int J Mol Sci. 2025 Jan 14;26(2):649. doi: 10.3390/ijms26020649.

(2) Li K, Ling H, Wang X, Xie Q, Gu C, Luo W, Qiu P. The role of NF-κB signaling pathway in reactive astrocytes among neurodegeneration after methamphetamine exposure by integrated bioinformatics. Prog Neuropsychopharmacol Biol Psychiatry. 2024 Feb 8;129:110909. doi: 10.1016/j.pnpbp.2023.110909.

(3) Wu L, Liu X, Jiang Q, Li M, Liang M, Wang S, Wang R, Su L, Ni T, Dong N, Zhu L, Guan F, Zhu J, Zhang W, Wu M, Chen Y, Chen T, Wang B. Methamphetamine-induced impairment of memory and fleeting neuroinflammation: Profiling mRNA changes in mouse hippocampus following short-term and long-term exposure. Neuropharmacology. 2024 Dec 15;261:110175. doi: 10.1016/j.neuropharm.2024.110175.

> *(3) The conclusion that "prolonged METH use may progressively impair cognitive function" may not be uniformly supported by the behavioral data: Figures 1C and F (discrimination and preference indexes) exhibited that the 4-week test further declined in the METH group compared to the 2-week. In contrast, Figure 1E and H present a contradictory pattern.*

Thank you very much for pointing this out. Your observation is very detailed and constructive. Regarding the conclusion "prolonged use of METH may progressively impair cognitive function", our main basis is the discrimination index and preference index shown in Figures 1C and 1F. These two indicators are usually calculated based on the total exploration time of new and old objects by mice. They are widely adopted as important references for cognitive function assessment in many relevant literature [1-3], thus providing strong support for our conclusion. The exploration frequency data we provided can, on the one hand, reflect the curiosity of mice towards new things, and on the other hand, can be calculated as the average time of each exploration by "total exploration time / exploration frequency", thereby evaluating their learning interest and the degree of their focus during exploration. We believe this is also of certain significance for reflecting the effect of METH on learning. As for the fact that there is no statistically significant difference in the exploration frequency of new and old objects in the 4-week-old mice in Figure 1H, we are also regretful about this. This might be due to the fact that our tests allow mice to freely explore in a stress-free environment, and there are significant differences among individual mice within the group. However, the mean values still show certain differences between the two groups. Compared to the mice at 2 weeks, the mice at 4 weeks have undergone a NOR test once and may have formed memories, which were retained in the subsequent assessment after four weeks. Moreover, we believe that injecting normal saline to the control group mice for a long time may affect their emotional state, because they cannot obtain the same pleasure as that brought by METH from the injection behavior.

(1) Riva M, Moriceau S, Morabito A, Dossi E, Sanchez-Bellot C, Azzam P, Navas-Olive A, Gal B, Dori F, Cid E, Ledonne F, David S, Trovero F, Bartolomucci M, Coppola E, Rebola N, Depaulis A, Rouach N, de la Prida LM, Oury F, Pierani A. Aberrant survival of hippocampal Cajal-Retzius cells leads to memory deficits, gamma rhythmopathies and susceptibility to seizures in adult mice. Nat Commun. 2023 Mar 18;14(1):1531. doi: 10.1038/s41467-023-37249-7.

(2) Lu Y, Chen X, Liu X, Shi Y, Wei Z, Feng L, Jiang Q, Ye W, Sasaki T, Fukunaga K, Ji Y, Han F, Lu YM. Endothelial TFEB signaling-mediated autophagic disturbance initiates microglial activation and cognitive dysfunction. Autophagy. 2023 Jun;19(6):1803-1820. doi: 10.1080/15548627.2022.2162244.

(3) Arroyo-García LE, Tendilla-Beltrán H, Vázquez-Roque RA, Jurado-Tapia EE, Díaz A, Aguilar-Alonso P, Brambila E, Monjaraz E, De La Cruz F, Rodríguez-Moreno A, Flores G. Amphetamine sensitization alters hippocampal neuronal morphology and memory and learning behaviors. Mol Psychiatry. 2021 Sep;26(9):4784-4794. doi: 10.1038/s41380-020-0809-2.

https://doi.org/10.7554/eLife.106940.2.sa0